

# Numerical gradient flow discretization of viscous thin films on curved geometries

Martin Rumpf, Orestis Vantzos

## Abstract

The evolution of a viscous thin film on a curved geometry is numerically approximated based on the natural time discretization of the underlying gradient flow. This discretization leads to a variational problem to be solved at each time step, which reflects the balance between the decay of the free (gravitational and surface) energy and the viscous dissipation. Both dissipation and energy are derived from a lubrication approximation for a small ratio between the characteristic film height and the characteristic length scale of the surface. The dissipation is formulated in terms of a corresponding flux field, whereas the energy primarily depends on the fluid volume per unit surface, which is a conserved quantity. These two degrees of freedom are coupled by the underlying transport equation. Hence, one is naturally led to a PDE-constrained optimization problem, where the variational time stepping problem has to be solved under the constraint described by the transport equation. For the space discretization a discrete exterior calculus approach is investigated. Various applications demonstrate the qualitative and quantitative behavior of one and two dimensional thin films on curved geometries.

**Keywords:** Viscous thin film; gradient flow; variational time discretization; PDE-constraint optimization; discrete exterior calculus.

## 1 Introduction

During recent years, the investigation of the dynamics of liquid thin films has attracted increased attention in the field of physics, engineering and mathematics. In many applications in materials science and biology, liquid thin films do not reside on a flat Euclidean domain but on curved surfaces (Howell[25], Roy, Roberts and Simpson[39], Schwartz and Weidner[41], Wang[46]). Examples are the spreading of liquid coatings on surfaces, the surfactant-driven thin film flow on the interior of the lung alveoli (Xu *et al.*[47]) and the tear film on the cornea of the eye (Braun *et al.*[9]). The evolution of the film thickness is often of greater interest than the actual velocity or pressure field within the fluid volume. In that case, a lubrication approximation dating back already to Reynolds[37] allows us to replace the governing Navier-Stokes and moving free boundary model with an evolution model expressed solely in terms of the film height or a related quantity. For a thin film deposited on a planar substrate, and

in the limit of vanishing thickness-to-length ratio, one can derive through the well-known lubrication theory (Oron, Davis and Bankoff[34]) a limit model in the form of a fourth order nonlinear parabolic problem for the evolution of the film height  $h$  (Bernis and Friedman[5], Bertozzi and Pugh[6], Bernis[4], Beretta, Bertsch and Dal Paso[3]). We refer to Oron, Davis, and Bankoff[34] for the derivation of the model and to Myers[31] for an overview of the mathematical treatment of surface-tension-driven thin fluid films. A recent review by Craster and Matar[10] discusses the dynamics and stability of thin liquid films involving external forcing, thermal effects and intermolecular forces.

Already in '84, Wang[46] presented a lubrication model for the evolution of a thin film flowing down a curved surface. Schwartz and Weidner[41] discussed the additional forcing effect due to the surface curvature. A lubrication model for the dynamics of the film, in the form of a PDE for the evolution of the film thickness, has been derived by Roy, Roberts and Simpson[39]. Unlike the case of a flat substrate, their lubrication model is an approximation of the Navier-Stokes equations, rather than the limit model for vanishing film thickness. The approximation is based on a second order expansion in  $\epsilon$ , where  $\epsilon$  is the scale ratio between the characteristic height of the film and the characteristic length of the surface. In Section 2 we recall the essential ingredients of this derivation. Roberts and Li[38] extended this model to include inertial effects, by adding an evolution law for the average lateral velocity. In Thiffeault and Kamhawi[44] gravity-driven thin film flows on curved substrates are studied from a dynamical systems point of view. A related gravity-driven shallow water model on curved geometries, namely topographic maps, was investigated by Boutounet *et al.*[7] Kalliadasis and Bielarz[27] directly applied a thin film model on topographic maps to analyze the impact of topological features on the formation of capillary ridges. Jensen *et al.*[26] studied the flow of a thin, homogeneous liquid layer induced by a sudden change in the shape of the substrate. Thin film flow on moving curved surfaces was investigated by Howell[25], who explored the behavior for large, non-uniform curvature, whose gradient dominates the flow and leads in the limit to a hyperbolic equation with shock formation at specific regions of the substrate. The flow of a thin film on a flat, but non-linearly stretching, sheet was discussed by Santra and Dandapat[40].

Convergent numerical discretizations of thin film flow were investigated for instance by Zhornitskaya and Bertozzi[49] using an entropy-consistent finite difference scheme, and independently by Grün and Rumpf[21] based on a related finite element approach. A numerical discretization of surfactant spreading on liquid thin films was proposed and analyzed by Barrett *et al.*[1]. For the discretization of the thin film equation on curved substrates, Roy, Roberts and Simpson[39] used a straightforward finite difference approximation of the fourth order PDE with implicit treatment of the higher order terms and a small ratio of time step to spatial grid size to cope with the stiffness of the problem. Schwartz and Weidner also applied a semi-implicit finite difference scheme and Myers *et al.*[32] used a semi-implicit finite volume type approach with a flux splitting. A level set implementation of the model in Roy, Roberts and Simpson[39] was proposed by Greer *et al.*[20] To ensure the stability of the proposed schemes in

all these cases, the time step size has to be chosen very small. A variational time discretization of the underlying gradient flow structure, such as the one presented in this paper, offers an attractive alternative and in particular allows for large time steps.

In this work, we explore the gradient flow structure of the evolution of a liquid thin film on a fixed curved surface, we use this structure to derive a natural time discretization and, together with techniques from discrete exterior calculus, we develop it into a robust and efficient simulation tool. The gradient flow structure has already been investigated in the context of the analysis of the thin film equation on planar domains by, among others, Otto[35], Giacomelli and Otto[18, 17], Mattes *et al.*[30] and Slepčev[42]. In abstract terms, a gradient flow  $\frac{d}{dt}x = -\text{grad}_g e[x]$  describes the evolution of a state  $x$  in the direction of the negative gradient of an energy  $e[\cdot]$  with respect to a given metric  $g$  on the space of states. The gradient of the energy  $e$  at a state  $x$  is defined as the representation of the variation of the energy  $e'[x]$  in the metric, i. e.  $g(\text{grad}_g e[x], \theta) = e'[x](\theta)$  for all state variations  $\theta$  of  $x$ . It follows that we can rewrite the gradient flow as  $g(\frac{d}{dt}x, \theta) = -e'[x](\theta)$  for all  $\theta$ . Applied to thin films, the gradient flow structure naturally represents the balance between the kinetic effect of viscous dissipation due to friction in the fluid (on the left-hand side) and the rate of change of the surface energy (on the right-hand side). As in Roy, Roberts and Simpson[39], we neglect the inertia of the fluid and assume an over-damped limit in which the quasi-stationary Stokes equations for an incompressible fluid are appropriate. Furthermore, we only consider thin film layers of strictly positive thickness together with the no-slip condition at the fluid-substrate interface.

Every gradient flow  $\frac{d}{dt}x = -\text{grad}_g e[x]$ , for a given energy functional  $e$  and underlying metric  $g$ , has a natural time discretization (Otto[35]). It involves the distance function  $\text{dist}(\cdot, \cdot)$  on the space of states, which is induced by the metric  $g$ . If  $\tau$  denotes the time step size, a time-discrete state  $x^{k+1}$  at time  $t_{k+1} = t_k + \tau$  can be inferred from the state  $x^k$  at time  $t_k$  via the variational problem

$$x^{k+1} = \underset{x}{\operatorname{argmin}} \left\{ \frac{1}{2\tau} \text{dist}^2(x^k, x) + e[x] \right\}.$$

In the case of thin films on curved surfaces, the state  $x$  is given by the mass distribution  $u$  of the liquid layer, whereas the distance term measures the viscous dissipation caused by an optimal transport of mass within the time step. The above variational problem can therefore be viewed as an optimization problem with a PDE constraint given by the transport equation for the mass distribution. In this paper we derive a robust discretization scheme based on this variational formulation. To this end, we approximate the squared distance via a quadrature rule involving the metric  $g$  and obtain a semi-implicit optimization problem for the mass distribution  $u$  at time  $t^{k+1}$  and a flux quantity  $f$ , where  $u$  and  $f$  are coupled via a time-discrete conservation law. For planar surfaces and thin coatings consisting of a resin and a solvent component, such a scheme has already been investigated by Dohmen *et al.*[12] Düring *et al.*[13] also derived a numerical scheme for a fourth order PDE using an underlying gradient flow

structure. Similar to our approach, they applied direct numerical integration of the underlying Wasserstein-type transport problem for the nonlinear fourth order Derrida-Lebowitz-Speer-Spohn equation. Glasner[19] used a Galerkin discretization of a variational model related to ours to study the movement of the contact lines of thin films on planar substrates.

To define space-discrete counterparts of the dissipation and energy functionals and the transport PDE on curved geometries, we make use of the concept of discrete exterior calculus as proposed by Marsden and coworkers. For a comprehensive introduction we refer to the PhD thesis of Hirani[23]. An overview is given in Desbrun *et al.*[11]. The use of discrete differential forms (Desbrun, Kanso and Tong[11]) leads to consistent discretization schemes on triangulated approximations of the geometry. This approach has been successfully applied to models such as the Darcy flow (Hirani, Nakshatrala and Chaudhry[24]) and the Navier-Stokes equations (Elcott *et al.*[14, 15]).

In 'first discretize, then optimize' fashion, we follow the general theory of PDE-constrained optimization to minimize the fully (space- and time-) discrete functional at every time step. As we document below, the resulting scheme turns out to be very stable in practice and allows for very large time steps.

## 2 Derivation of the Gradient Flow Model

The flow of a thin film on a curved substrate is determined by the interplay between the viscous dissipation, caused by friction within the liquid film layer, and the energy given by the integrated surface tension on the liquid-gas interface and the potential energy due to gravity. Let us first outline the derivation of the gradient flow model. Compared to the exposition in Roy, Roberts and Simpson[39], we aim here at the derivation of appropriate dissipation and energy functionals instead of a governing PDE, and we express them in terms of a flux and a mass concentration variable instead of the film height. Thereby, we will apply an expansion in terms of the scale ratio  $\epsilon$  between the characteristic height of the film and the characteristic length on the surface.

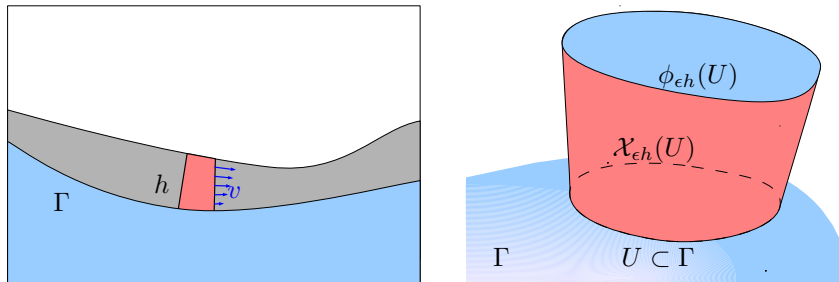


Figure 1: *Thin film on curved substrate.* Sketch of thin film on [Left] 1D and [Right] 2D substrates.

Fig. 1 sketches the geometric configuration in the case of a thin film on 1D

and 2D substrates. In this section, we derive a thin film model for a smooth two-dimensional surface  $\Gamma$ ; the derivation of the corresponding one-dimensional model follows along similar lines. We assume that the surface  $\Gamma$  is embedded in  $\mathbb{R}^3$  through the map  $\phi_0 : \Gamma \mapsto \mathbb{R}^3$ . Moreover, the mapping  $\phi_0$  is assumed *isometric*, i.e.  $\langle v, w \rangle_\Gamma = \langle d\phi_0(v), d\phi_0(w) \rangle$  for any  $v, w \in T\Gamma$ , where  $d\phi_0$  is the differential of  $\phi_0$ , and  $\langle \cdot, \cdot \rangle_\Gamma$  and  $\langle \cdot, \cdot \rangle$  are the inner products in  $T\Gamma$  and  $\mathbb{R}^3$ , respectively, with  $|\cdot|_\Gamma = \sqrt{\langle \cdot, \cdot \rangle_\Gamma}$  denoting the associated norm on  $T\Gamma$ . For a function  $f : \Gamma \mapsto \mathbb{R}$  on the substrate surface  $\Gamma$ , we define the (normal) displacement map  $\phi_f : \Gamma \mapsto \mathbb{R}^3$  as  $\phi_f(x) := \phi_0(x) + f(x)n(x)$ , where  $n(x)$  is the unit normal vector on  $\Gamma$ . For a subset  $U \subseteq \Gamma$ ,  $\phi_f(U)$  is its image under  $\phi_f$  and the extrusion of  $U$  under  $\phi_f$  is defined as  $\mathcal{X}_f(U) := \bigcup_{\xi=0}^1 \phi_{\xi f}(U)$ .

In fact, we assume that the thin film is an extrusion of the substrate of the form  $\mathcal{X}_{\epsilon h}(\Gamma)$ , where  $0 < \epsilon \ll 1$  and  $h(\cdot, t)$  is a rescaled, time-dependent height function on  $\Gamma$ . In this paper we assume that  $h$  is strictly positive. The motion of the film is driven by the velocity field  $v$  of the (incompressible and Newtonian) fluid, which is assumed to satisfy the Stokes equations (*creeping flow*) in  $\mathcal{X}_{\epsilon h}(\Gamma)$ , with a no-slip boundary condition at the liquid-solid interface  $\phi_0(\Gamma)$  and a free boundary representing the liquid-gas interface at  $\phi_{\epsilon h}(\Gamma)$ .

In the derivation of the model, the mapping

$$\phi : \Gamma \times \mathbb{R} \rightarrow \mathbb{R}^3; (x, \xi) \mapsto \phi_0(x) + \epsilon \xi n(x) \quad (1)$$

plays a prominent role, since it can be used to cover the fluid domain  $\mathcal{X}_{\epsilon h}(\Gamma) \subset \mathbb{R}^3$  with a  $\xi$ -parametrized family of images of  $\Gamma$ . The differential of  $\phi$  can be written as  $d\phi(\delta x, \delta \xi) = d\phi_0(\Lambda \delta x) + \epsilon \delta \xi n(x)$ , for  $(\delta x, \delta \xi) \in T\Gamma \times \mathbb{R}$  with  $\Lambda := \text{id} - \epsilon \xi S$ . Here  $S$  denotes the shape operator of  $\Gamma$ , which is a symmetric endomorphism on the tangent bundle of  $\Gamma$  defined via  $d\phi_0(S\delta x) = -D_{\delta x}n$ , where  $D_{\delta x}n$  denotes the directional derivative of  $n$  in the direction of  $\delta x$ . We assume that the parameter  $\epsilon > 0$  and the values of the height function  $h$  are small enough, so that  $\det \Lambda > 0$  for all  $0 \leq \xi \leq h$  and the Jacobian of  $\phi$  is nowhere singular on  $\mathcal{X}_{\epsilon h}(\Gamma)$ . It follows that for any point  $p \in \mathcal{X}_{\epsilon h}(\Gamma)$ , there is a unique  $(x, \xi) \in \Gamma \times \mathbb{R}$  so that  $p = \phi(x, \xi)$ . Furthermore, for a vector field  $v$  on  $\mathcal{X}_{\epsilon h}$  we can consider its decomposition into a tangential  $v_\Gamma(x, \xi) \in T\Gamma$  and a normal component  $v_n(x, \xi) \in \mathbb{R}$ , determined by

$$v(\phi(x, \xi)) = d\phi_0(v_\Gamma(x, \xi)) + v_n(x, \xi)n(x). \quad (2)$$

Regarding the scaling of the various quantities in the rest of the section, we assume that there is a length scale  $L$  on  $\Gamma$  and a length scale  $H = \epsilon L$  in the normal direction, so that  $\xi \sim H$ . The characteristic time scale is  $T = \frac{\mu L}{\sigma} \epsilon^{-2}$ , where  $\mu$  is the viscosity and  $\sigma$  the surface tension constant, and the characteristic (tangential) velocity is  $V = \frac{L}{T} = \frac{\sigma}{\mu} \epsilon^2$ . In what follows, we will assume that a rescaling with  $L^{-1}$  is already incorporated in the description of the surface  $\Gamma$ . Note that the choice of the time scale implies that the (dimensionless) capillary number  $\frac{\mu V}{\sigma}$ , which measures the relative strength of viscous and capillary forces, should scale like  $\epsilon^2$  and therefore be small.

## 2.1 Conservation law

The evolution of the thin film follows a conservation law that can be expressed in terms of a mass distribution and a flux. Normalizing the density to 1, the mass distribution  $u : \Gamma \mapsto \mathbb{R}$  represents the fluid volume per unit area and satisfies  $\int_{\mathcal{X}_{\epsilon h}(U)} dV = \epsilon \int_U u \, da$  for all  $U \subset \Gamma$ . From this, we deduce that  $u = \int_0^h \lambda \, d\xi$  where  $\lambda := \det \Lambda$ . If  $\kappa_1$  and  $\kappa_2$  are the principal curvatures of  $S$ , we have that  $\lambda = \det(\text{id} - \epsilon \xi S) = (1 - \epsilon \xi \kappa_1)(1 - \epsilon \xi \kappa_2) = 1 - \epsilon \xi H + \epsilon^2 \xi^2 K$ , where  $H, K$  denote the mean and Gaussian curvature, respectively. It follows that  $u = h - \frac{\epsilon}{2} H h^2 + \frac{\epsilon^2}{3} K h^3$  and conversely

$$h = u + \frac{\epsilon}{2} H u^2 + \mathcal{O}(\epsilon^2). \quad (3)$$

The flux  $F$  is a tangential vector field on  $\Gamma$ , uniquely described by  $\int_{\mathcal{X}_{\epsilon h}(\partial U)} \langle v, \mathbf{n} \rangle \, da = \epsilon \int_{\partial U} \langle F, \nu \rangle_{\Gamma} \, dl$  for any  $U \subset \Gamma$  with a smooth boundary  $\partial U$ . The vectors  $\mathbf{n}$  and  $\nu$  denote the unit normal of  $\mathcal{X}_{\epsilon h}(\partial U)$  and the unit conormal of  $\partial U$  respectively. The flux represents the total flow of mass induced by the flow field  $v$ , integrated in the normal direction. Using once more the mapping  $\phi$ , we can show that  $F = \int_0^h \text{cof} \Lambda \, v_{\Gamma} \, d\xi$ , where  $v_{\Gamma}$  is the tangential component of  $v$ , defined as in (2), and  $\text{cof} \Lambda = \lambda \Lambda^{-T} = \lambda \Lambda^{-1}$ . Finally, given the mass distribution  $u$  and the flux  $F$ , we obtain the transport PDE

$$\frac{\partial u}{\partial t} + \text{div}_{\Gamma} F = 0,$$

which reflects mass conservation in the thin film. We also introduce the partial flux  $\mathfrak{F}$ , defined as  $\mathfrak{F}(\xi) = \int_0^{\xi} \text{cof} \Lambda \, v_{\Gamma} \, d\xi$  so that  $F = \mathfrak{F}(h)$  and  $v_{\Gamma} = \text{cof} \Lambda^{-1} \frac{\partial \mathfrak{F}}{\partial \xi}$ .

## 2.2 Dissipation and mobility

The rate of viscous dissipation due to friction within the (incompressible and Newtonian) liquid film is given by  $2\mu \int_{\mathcal{X}_{\epsilon h}(\Gamma)} \|D[v]\|_F^2 \, dV$ , and is a function of the derivatives of the fluid velocity  $v$  in the fluid volume (Pozrikidis[36]). In this expression,  $\mu$  is the viscosity,  $D[v] = \frac{1}{2}(\nabla v + \nabla v^T)$  is the rate-of-strain tensor and  $\|A\|_F^2 := \text{tr}(A^T A)$  is the (squared) Frobenius norm. Following the approach by Roy, Roberts and Simpson[39], and using the expressions for the components of the rate-of-strain tensor in curvilinear coordinates found in the Appendix 2 of Batchelor[2], one observes that the components which correspond to the shear stress due to the laminar motion of the fluid dominate the other components of  $D[v]$ . Indeed, identifying the leading order terms in the asymptotic expansion of  $\|D[v]\|_F^2$  wrt  $\epsilon$  and scaling with the characteristic dissipation rate  $\frac{\sigma^2 L}{\mu} \epsilon^3$ , we obtain the dimensionless dissipation

$$\mathfrak{g}(v, v) = \int_{\Gamma} \int_0^h \left| \frac{\partial v_{\Gamma}}{\partial \xi} + \epsilon S v_{\Gamma} \right|_{\Gamma}^2 \lambda \, d\xi \, da + \mathcal{O}(\epsilon^2). \quad (4)$$

A detailed exposition is given in A below (cf. also the derivation of the lubrication model in the flat case by Oron, Davis and Bankoff[34]). Next, we perform a model reduction through partial optimization and assume that for given boundary conditions at the liquid-solid and the liquid-gas interface the velocity profile in normal direction will adjust to minimize the resulting dissipation. This allows us to express the rate of dissipation in terms of the total flux  $F$  as explained in what follows.

Noting that  $\epsilon S = -\frac{\partial \Lambda}{\partial \xi}$  and that  $\Lambda$  is a symmetric matrix, we can rewrite the dissipation integrated in the normal direction as

$$\begin{aligned} & \int_0^h \left| \frac{\partial v_\Gamma}{\partial \xi} - \frac{\partial \Lambda}{\partial \xi} v_\Gamma \right|_\Gamma^2 \lambda \, d\xi = \int_0^h \lambda \left| e^\Lambda \frac{\partial}{\partial \xi} (e^{-\Lambda} v_\Gamma) \right|_\Gamma^2 \, d\xi \\ & = \int_0^h \lambda \left| e^\Lambda \frac{\partial}{\partial \xi} \left( e^{-\Lambda} \operatorname{cof} \Lambda^{-1} \frac{\partial \mathfrak{F}}{\partial \xi} \right) \right|_\Gamma^2 \, d\xi = \int_0^h \left\langle \frac{\partial}{\partial \xi} \left( B(\Lambda) \frac{\partial \mathfrak{F}}{\partial \xi} \right), A(\Lambda) \frac{\partial}{\partial \xi} \left( B(\Lambda) \frac{\partial \mathfrak{F}}{\partial \xi} \right) \right\rangle_\Gamma \, d\xi, \end{aligned}$$

where  $A(\Lambda) := \lambda e^{2\Lambda}$  and  $B(\Lambda) := e^{-\Lambda} \operatorname{cof} \Lambda^{-1}$ . Integrating by parts twice, we obtain for two partial flux functions  $\mathfrak{F}$  and  $\tilde{\mathfrak{F}}$

$$\begin{aligned} & \int_0^h \left\langle \frac{\partial}{\partial \xi} \left( B(\Lambda) \frac{\partial \tilde{\mathfrak{F}}}{\partial \xi} \right), A(\Lambda) \frac{\partial}{\partial \xi} \left( B(\Lambda) \frac{\partial \mathfrak{F}}{\partial \xi} \right) \right\rangle_\Gamma \, d\xi \\ & = \left[ \left\langle B(\Lambda) \frac{\partial \tilde{\mathfrak{F}}}{\partial \xi}, A(\Lambda) \frac{\partial}{\partial \xi} \left( B(\Lambda) \frac{\partial \mathfrak{F}}{\partial \xi} \right) \right\rangle_\Gamma - \left\langle \tilde{\mathfrak{F}}, B(\Lambda) \frac{\partial}{\partial \xi} \left( A(\Lambda) \frac{\partial}{\partial \xi} \left( B(\Lambda) \frac{\partial \mathfrak{F}}{\partial \xi} \right) \right) \right\rangle_\Gamma \right]_0^h \\ & \quad + \int_0^h \left\langle \tilde{\mathfrak{F}}, \frac{\partial}{\partial \xi} \left( B(\Lambda) \frac{\partial}{\partial \xi} \left( A(\Lambda) \frac{\partial}{\partial \xi} \left( B(\Lambda) \frac{\partial \mathfrak{F}}{\partial \xi} \right) \right) \right) \right\rangle_\Gamma \, d\xi. \end{aligned} \tag{5}$$

Now we ask for the profile of the partial flux  $\mathfrak{F}$  which minimizes the integral of the dissipation in the normal direction, under the boundary conditions  $\mathfrak{F}(0) = 0$ ,  $\mathfrak{F}(h) = F$ ,  $\mathfrak{F}'(0) = 0$  (no slip), and  $\frac{\partial}{\partial \xi} \left( B(\Lambda) \frac{\partial \mathfrak{F}}{\partial \xi} \right) \Big|_{\xi=h} = 0$  (zero shear stress at the liquid-gas interface). As a necessary condition for the optimality of  $\mathfrak{F}$  one achieves

$$0 = \int_0^h \left\langle \frac{\partial}{\partial \xi} B(\Lambda) \frac{\partial \delta \mathfrak{F}}{\partial \xi}, A(\Lambda) \frac{\partial}{\partial \xi} B(\Lambda) \frac{\partial \mathfrak{F}}{\partial \xi} \right\rangle_\Gamma \, d\xi, \tag{6}$$

for a variation  $\mathfrak{F} + \delta \mathfrak{F}$  of the partial flux  $\mathfrak{F}$ , for which the boundary conditions imply  $\delta \mathfrak{F}(0) = \delta \mathfrak{F}(h) = \frac{\partial \delta \mathfrak{F}}{\partial \xi}(0) = 0$ . Choosing  $\tilde{\mathfrak{F}} = \delta \mathfrak{F}$ , we observe that the boundary terms in (5) vanish and hence

$$0 = \int_0^h \left\langle \delta \mathfrak{F}, \frac{\partial}{\partial \xi} \left( B(\Lambda) \frac{\partial}{\partial \xi} \left( A(\Lambda) \frac{\partial}{\partial \xi} \left( B(\Lambda) \frac{\partial \mathfrak{F}}{\partial \xi} \right) \right) \right) \right\rangle_\Gamma \, d\xi$$

holds for all admissible variations  $\delta \mathfrak{F}$  of the profile. Consequently

$$f := - \left( B(\Lambda) \frac{\partial}{\partial \xi} \left( A(\Lambda) \frac{\partial}{\partial \xi} \left( B(\Lambda) \frac{\partial \mathfrak{F}}{\partial \xi} \right) \right) \right) \tag{7}$$

is constant in  $\xi$ . Next, integrating in the normal direction and using the boundary conditions gives

$$\begin{aligned} A(\Lambda) \frac{\partial}{\partial \xi} \left( B(\Lambda) \frac{\partial \mathfrak{F}}{\partial \xi} \right) &= \left( \int_{\xi}^h B(\Lambda_a)^{-1} da \right) f \Rightarrow \\ B(\Lambda) \frac{\partial \mathfrak{F}}{\partial \xi} &= \left( \int_0^{\xi} A(\Lambda_b)^{-1} \int_b^h B(\Lambda_a)^{-1} da db \right) f \Rightarrow \\ \mathfrak{F} &= \left( \int_0^{\xi} B(\Lambda_c)^{-1} \int_0^c A(\Lambda_b)^{-1} \int_b^h B(\Lambda_a)^{-1} da db dc \right) f, \end{aligned}$$

where  $\Lambda_r$  denotes  $\Lambda$  evaluated at  $\xi = r$ . Finally, having identified the optimal profile  $\mathfrak{F}$  in the normal direction, we can now rewrite the associated dissipation. Once more due to the boundary condition, (6) and (7), the only remaining term on the righthand side of (5) for  $\tilde{\mathfrak{F}} = \mathfrak{F}$  is

$$-\left\langle \mathfrak{F}(h), B(\Lambda) \frac{\partial}{\partial \xi} \left( A(\Lambda) \frac{\partial}{\partial \xi} \left( B(\Lambda) \frac{\partial \mathfrak{F}}{\partial \xi} \right) \right) \right\rangle_{\Gamma} = -\langle \mathfrak{F}(h), -f \rangle_{\Gamma} = \langle \mathfrak{M}(h)f, f \rangle_{\Gamma},$$

with  $F = \mathfrak{F}(h) = \mathfrak{M}(h)f$  and the mobility

$$\mathfrak{M}(h) := \int_0^h B(\Lambda_c)^{-1} \left( \int_0^c A(\Lambda_b)^{-1} \left( \int_b^h B(\Lambda_a)^{-1} da \right) db \right) dc. \quad (8)$$

Using the approximations

$$\begin{aligned} A(\Lambda)^{-1} &= \lambda^{-1} e^{-2\Lambda} = e^{-2}(\text{id} + \epsilon \xi (H \text{id} + 2S)) + \mathcal{O}(\epsilon^2) \\ B(\Lambda)^{-1} &= e^{\Lambda} \text{cof} \Lambda = e(\text{id} - \epsilon \xi H \text{id}) + \mathcal{O}(\epsilon^2), \end{aligned}$$

we can carry out the integrations in the definition of  $\mathfrak{M}(h)$  and obtain  $\mathfrak{M}(h) = \frac{h^3}{3} + \frac{\epsilon}{6} h^4 (S - 2H \text{id}) + \mathcal{O}(\epsilon^2)$ . Finally taking into account (3), we arrive at the following (approximate) mobility in terms of the mass distribution  $u$ :

$$M(u) := \frac{u^3}{3} + \frac{\epsilon}{6} u^4 (H \text{id} + S) \quad (9)$$

with  $M(u) = \mathfrak{M}(h) + \mathcal{O}(\epsilon^2)$ . Thus, the dissipation acting on a flux  $f$  is given by

$$g_u(f, f) := \int_{\Gamma} \langle f, M(u)f \rangle_{\Gamma} da \quad (10)$$

and  $g_u(f, f) = \mathbf{g}(v, v) + \mathcal{O}(\epsilon^2)$ . Furthermore, we conclude that the transport equation can be written as

$$\frac{\partial u}{\partial t} + \text{div}_{\Gamma}(M(u)f) = 0, \quad (11)$$

where the flux  $f$  is related to the actual physical flux  $F$  via  $F = \mathfrak{M}(h)f$ .

### 2.3 Energy

We can express the total (dimensionless) energy of the thin film, in the presence of gravity and surface tension, as

$$\mathfrak{E}(u) = \mathfrak{E}_{gravity} + \mathfrak{E}_{surface} = \epsilon^{-1} \int_{\mathcal{X}_{\epsilon h}(\Gamma)} \zeta \mathbf{z} dV + \epsilon^{-1} \int_{\phi_{\epsilon h}(\Gamma)} da,$$

where  $\zeta := \frac{\rho g L^2}{\sigma}$  is the Bond number, which represents the relative effect of gravity versus surface tension,  $\rho$  is the density and  $g$  the gravity constant. The Cartesian coordinate  $\mathbf{z}$  in  $\mathbb{R}^3$  is chosen such that  $\hat{g} := -\nabla \mathbf{z}$  represents the (constant) unit vector in the direction of gravity. We note that the characteristic energy is  $\epsilon \sigma L^2$ . Furthermore, we allow the values of  $\mathbf{z}$  in  $\mathcal{X}_{\epsilon h}(\Gamma)$  to scale like the horizontal length scale  $L$ , unlike in the classic case of a slightly inclined plane where  $\mathbf{z}$  scales like the vertical length scale  $H$  (i.e. the film is almost horizontal).

The first integral can be written as

$$\begin{aligned} \frac{1}{\epsilon} \int_{\mathcal{X}_{\epsilon h}(\Gamma)} \zeta \mathbf{z} dV &= \int_{\Gamma} \int_0^h \zeta(\mathbf{z}(\phi(x, \xi))) \lambda(x, \xi) d\xi da(x) \\ &= \int_{\Gamma} \int_0^h \zeta(\mathbf{z}(\phi_0(x)) + \epsilon \xi \langle \nabla \mathbf{z}(\phi_0(x)), n(x) \rangle + O(\epsilon^2)) \lambda(x, \xi) d\xi da(x) \\ &= \int_{\Gamma} \zeta \left( zu + \epsilon \frac{u^2}{2} \cos \theta + O(\epsilon^2) \right) da, \end{aligned} \quad (12)$$

where  $\cos \theta(x) := \langle \nabla \mathbf{z}(\phi_0(x)), n(x) \rangle = -\langle \hat{g}, n(x) \rangle$  and  $z := \mathbf{z} \circ \phi_0$  is the pullback of  $\mathbf{z}$  onto  $\Gamma$  in the final integral and in the rest of this paper.

Now consider the free surface area  $A[h] := \int_{\phi_{\epsilon h}(\Gamma)} da$ . It is a classic result of the differential geometry of surfaces in  $\mathbb{R}^3$ , that the first variation of the area functional under normal variations like  $\phi_{\epsilon h}$  is given by  $A'[0](h) = -\int_{\Gamma} H h da$ , and the second variation of the area functional under normal variations is shown to be  $A''[0](h) = \int_{\Gamma} 2K h^2 + |\text{grad}_{\Gamma} h|_{\Gamma}^2 da$ . (cf. Nitsche[33] §101, §103). Given the first and second variation of  $A[h]$ , we obtain the following expansion

$$A[h] = A[0] + \epsilon A'[0](h) + \frac{\epsilon^2}{2} A''[0](h) + O(\epsilon^3)$$

in the parameter  $\epsilon$ . Based on this expansion, and substituting  $h$  for  $u$  using (3), we arrive at the approximation

$$\frac{1}{\epsilon} \int_{\phi_{\epsilon h}(\Gamma)} da = \frac{1}{\epsilon} \int_{\Gamma} da + \int_{\Gamma} -H u - \frac{\epsilon}{2} T u^2 + \frac{\epsilon}{2} |\text{grad}_{\Gamma} u|_{\Gamma}^2 da + O(\epsilon^2), \quad (13)$$

where  $T := H^2 - 2K = \kappa_1^2 + \kappa_2^2$ . The leading order term is constant since  $\Gamma$  is fixed, and therefore does not contribute to the dynamics of the thin film. Summing the second term in (13) with the gravitational energy (12) we get the total energy functional

$$E[u] = \int_{\Gamma} (\zeta z - H) u + \frac{\epsilon}{2} (\zeta \cos \theta - T) u^2 + \frac{\epsilon}{2} |\text{grad}_{\Gamma} u|_{\Gamma}^2 da \quad (14)$$

used in our model, with  $E[u] = \mathfrak{E}[u] + O(\epsilon^2)$ .

## 2.4 Gradient flow model

Once, we have derived first order approximations of the dissipation and the energy in terms of the characteristic ratio  $\epsilon$  we have all the ingredients at hand to discuss the lubrication approximation of the thin film gradient flow. Let us begin with an abstract notion of this flow

$$\partial_t u = -\text{grad}_{\tilde{g}} E[u], \quad (15)$$

where the metric  $\tilde{g}$  acts on admissible variations  $\delta u$  of the mass distribution  $u$  and  $\tilde{g}(\delta u, \delta u)$  represents the minimal physical dissipation required to generate the infinitesimal variation  $\delta u$ . By definition the gradient  $\text{grad}_{\tilde{g}} E[u]$  of the energy  $E$  evaluated for a mass distribution  $u$  is given as the representation of the derivative  $E'[u]$  of the energy  $E$  in the metric  $\tilde{g}$ . Thus, (15) can be rephrased as

$$0 = \tilde{g}_u(\partial_t u, \delta u) + E'[u](\delta u)$$

for infinitesimal variations  $\delta u$  of the mass distribution  $u$ . As derived in Section 2.2 the dissipation is best described in terms of the fluxes generating a given variation of the mass distribution. Hence, picking up the dissipation defined in (10) we define

$$\tilde{g}_u(\delta u, \delta u) := \min_{\delta u = -\text{div}(M(u)\delta f)} g_u(\delta f, \delta f),$$

where admissible variations  $\delta u$  of the mass distribution are those resulting from fluxes  $\delta f$  via the conservation law, i. e.  $\delta u = -\text{div}_{\Gamma}(M(u)\delta f)$ . Hence, we obtain for the gradient flow the representation

$$0 = g_u(f, \delta f) + E'[u](\delta u), \quad (16)$$

where  $\delta f$  is any infinitesimal variation of the flux  $f$  and  $\delta u$  the associated infinitesimal variation of the mass distribution  $u$ . For given  $u$  Eq. (16) determines the flux  $f$  and given  $f$  the underlying conservation law  $\partial_t u + \text{div}_{\Gamma}(M(u)f) = 0$  gives rise to the actual dynamics of the thin film. Let us remark that Eq. (16) also can be seen as the Euler Lagrange equation for a minimizer  $f$  of the corresponding to the Rayleigh functional  $\mathcal{R}(\delta f) := \frac{1}{2}g_u(\delta f, \delta f) + E'[u](\delta u)$  subject to the conservation law  $\delta u = -\text{div}_{\Gamma}(M(u)\delta f) = 0$  as a constraint.

A major difference from the flat case is that instead of the height  $h$  and the transport velocity  $v$ , we have the mass distribution  $u$  and a flux quantity  $f$ . Furthermore, the mobility  $M(u)$  is a tensor valued function of  $u$ , whereas in the flat case it is a scalar quantity. Finally the  $|\text{grad}_{\Gamma} u|_{\Gamma}^2$  term, which drives the dynamics in the case of a flat surface, is relegated to a first order correction in the presence of curvature.

Even though we intend to directly discretize the gradient flow via a natural time discretization, let us discuss briefly the associated PDE. Taking into account the underlying transport equation we deduce from (16) via integration by

parts

$$\begin{aligned} 0 &= \int_{\Gamma} \langle M(u)f, \delta f \rangle_{\Gamma} - E'[u] (\operatorname{div}_{\Gamma}(M(u)\delta f)) \, da \\ &= \int_{\Gamma} \langle M(u)f, \delta f \rangle_{\Gamma} + \langle \operatorname{grad}_{\Gamma} \frac{\delta E}{\delta u}, M(u)\delta f \rangle_{\Gamma} \, da \end{aligned}$$

for every flux variation  $\delta f$ , where  $\frac{\delta E}{\delta u}$  represents the  $L^2$  density of the energy variation  $E'[u]$ . Thus, we obtain  $f = -\operatorname{grad}_{\Gamma} \frac{\delta E}{\delta u}$ . Inserting this into the transport equation we achieve

$$\frac{\partial u}{\partial t} = \operatorname{div}_{\Gamma} \left( M(u) \operatorname{grad}_{\Gamma} \frac{\delta E}{\delta u} \right). \quad (17)$$

Indeed, this PDE coincides with the PDE model derived in Roy, Roberts and Simpson[39] up to a higher order term of the order of  $O(\epsilon^2)$ . Using the notation of this paper the PDE model of Roy, Roberts and Simpson can be rephrased as

$$\begin{aligned} \frac{\partial u}{\partial t} &= -\frac{1}{3} \operatorname{div}_{\Gamma} \left( h^2 u \operatorname{grad}_{\Gamma} \tilde{H}[u] - \frac{\epsilon}{2} h^4 (H \operatorname{id} - S) \operatorname{grad}_{\Gamma} H \right) \\ &\quad - \frac{\zeta}{3} \operatorname{div}_{\Gamma} \left( h^3 \hat{g}_{\Gamma} - \epsilon h^4 (H \operatorname{id} + \frac{1}{2} S) \hat{g}_{\Gamma} + \epsilon \hat{g}_n h^3 \operatorname{grad}_{\Gamma} h \right), \quad (18) \end{aligned}$$

where  $\tilde{H}[u] = H + \epsilon T u + \epsilon \Delta_{\Gamma} u + O(\epsilon^2)$  is the mean curvature of the free boundary and  $\hat{g}_{\Gamma}$ ,  $\hat{g}_n$  are the tangential and vertical components of the unit vector  $\hat{g}$  in the direction of gravity. We refer to B for the corresponding verification.

### 3 Discretization of the Gradient Flow

Instead of discretization the fourth order PDE (18) we aim for a variational time discretization of the gradient flow, which will be derived in the next section and then discretized also in space using a discrete exterior calculus approach on a triangulated approximation of the surface  $\Gamma$ .

#### 3.1 Natural time discretization of the gradient flow

Let us recall the natural time discretization of the thin film gradient flow in its abstract form introduced already in Section 1, i. e. given a mass distribution  $u^k$  on  $\Gamma$  at time  $t^k$ , we define the mass distributions  $u^{k+1}$  at time  $t^{k+1} = t^k + \tau$  as

$$u^{k+1} := \operatorname{argmin}_u \left\{ \frac{1}{2\tau} \operatorname{dist}^2(u_k, u) + E[u] \right\}$$

where the squared distance  $\operatorname{dist}^2(u_0, u_1)$  between two mass distributions  $u_0$  and  $u_1$  is defined as the minimal dissipation required to transport  $u_0$  into  $u_1$ . In case of (thick) fluid layers on  $\Gamma$  we obtain  $\operatorname{dist}^2(u_0, u_1) = \min_{\tilde{v}} \int_0^1 \mathbf{g}(\tilde{v}(s), \tilde{v}(s)) \, ds$ ,

where  $\tilde{v}$  is a motion velocity in the fluid volume and  $\mathbf{g}$  the associated dissipation by viscous friction given in (4). Here, the minimum is taken over all motion fields  $\tilde{v}$ , which transport the mass distribution  $u_0$  at time 0 through the path  $(\tilde{u}(s))_{s \in [0,1]}$  into the profile  $u_1$  at time 1. In Section 2.2 we have derived the first order expansion  $g_{\tilde{u}(s)}$  of the dissipation  $\mathbf{g}$  in the characteristic length ratio  $\epsilon$  for the lubrication approximation of a thin film flow. This directly leads us to the expansion  $\text{dist}^2(u_0, u_1) = \min_{(\tilde{u}, \tilde{f}) \in T_0^1[u_0, u_1]} \int_0^1 g_{\tilde{u}(s)}(\tilde{f}(s), \tilde{f}(s)) ds + O(\epsilon^2)$ , where  $T_{t_0}^{t_1}[u_0, u_1]$  is the set of solutions of the conservation law  $\partial_t \tilde{u} + \text{div}_\Gamma(M(\tilde{u})\tilde{f}) = 0$  with  $\tilde{u}(t_0) = u_0$  and  $\tilde{u}(t_1) = u_1$ . For  $M(u) = \text{const}$  this is directly related to the optimal transport of the concentration  $u_0$  to the concentration  $u_1$  (cf. Villani[45]). We will use this formal expansion as a starting point for a discretization in time. To this end, we rescale  $t = t^k + \tau s$  replacing in particular  $\tilde{u}(t)$  by  $\tilde{u}(s)$  and  $\tilde{f}(t)$  by  $\frac{1}{\tau}\tilde{f}(s)$  and obtain

$$\text{dist}^2(u_0, u_1) = \tau \min_{(\tilde{u}, \tilde{f}) \in T_{t^k}^{t^{k+1}}[u_0, u_1]} \int_{t^k}^{t^{k+1}} g_{\tilde{u}(t)}(\tilde{f}(t), \tilde{f}(t)) dt + O(\epsilon^2).$$

Finally, we choose  $u_0 = u^k$  at time  $t^k$  and  $u_1 = u$  at time  $t^{k+1}$  and obtain the natural discretization of the thin film gradient flow in the lubrication approximation, i. e. we ask for a mass distribution  $u^{k+1}$  which solves

$$\min_u \left\{ \frac{1}{2} \min_{(\tilde{u}, \tilde{f}) \in T_{t^k}^{t^{k+1}}[u^k, u]} \int_{t^k}^{t^{k+1}} g_{\tilde{u}(t)}(\tilde{f}(t), \tilde{f}(t)) dt + E[u] \right\}. \quad (19)$$

Thus, we end up with a PDE-constraint optimization problem, where the conservation law acts as the PDE-constraint coupling mass distribution  $\tilde{u}$  and flux  $\tilde{f}$  with prescribed data  $u^k$  and  $u$  at time  $t^k$  and  $t^{k+1}$ , respectively. To render the problem computationally feasible we replace in a first step the time integral over the dissipation by a simple quadrature rule and discretize the conservation law in time in a consistent way. Here, we confine to the explicit quadrature scheme  $\tau g_{u^k}(f, f) \approx \int_{t^k}^{t^{k+1}} g_{\tilde{u}(t)}(\tilde{f}(t), \tilde{f}(t)) dt$  of the dissipation functional with a constant in time approximation  $f$  of the flux  $\tilde{f}|_{[t^k, t^{k+1}]}$ . Furthermore, we consider the semi-implicit discretization  $\frac{u - u^k}{\tau} + \text{div}_\Gamma(M(u^k)f) = 0$  of the conservation law and finally end up with the time discrete and PDE-constraint variational problem

$$\min_{u, f} \left\{ \frac{\tau}{2} g_{u^k}(f, f) + E[u] \right\}, \quad (20a)$$

$$\text{where } u - u^k + \tau \text{div}_\Gamma(M(u^k)f) = 0. \quad (20b)$$

Let us remark that we obtain the same scheme via a straightforward discretization of the associated Lagrangian. Indeed, the Lagrangian of the above optimization problem is defined as

$$\mathcal{L}[u, f, p] := \frac{1}{2} \int_{t^k}^{t^{k+1}} g_u(f, f) dt + E[u(t^{k+1})] + \int_{t^k}^{t^{k+1}} \langle p, \partial_t u + \text{div}_\Gamma(M(u)f) \rangle dt$$

for space time continuous mass distribution  $u$  and flux  $f$  with a corresponding Lagrange multiplier  $p$  applied to the transport operator as the constraint and integrated in time. If one now discretizes  $u$  via piecewise linear and continuous mass distributions in time,  $f, p$  via piecewise constant fluxes in time, and uses the above quadrature rule one ends up with the same semi-implicit PDE-constraint variational problem. Let us mention, that Yoshimura and Marsden[48] proposed related quadrature based time discrete approximations in the context of conservative Hamiltonian systems.

### 3.2 Discretization of the geometry via DEC

In this section we derive a consistent space discretization of the proposed variational time stepping scheme based on the paradigms of discrete exterior calculus. We refer to the book by Frankel[16] for a comprehensive introduction into the underlying continuous exterior calculus and to Desbrun, Kato and Tong[11] and the PhD thesis of Hirani[23] for an overview of the corresponding discretization concepts. In our context the approach can equivalently be formulated as a finite volume method but in view of surfaces which themselves are only given as triangulations not resulting from the interpolation of a fixed smooth surface we consider the discrete exterior calculus approach as perspectivevely advantageous.

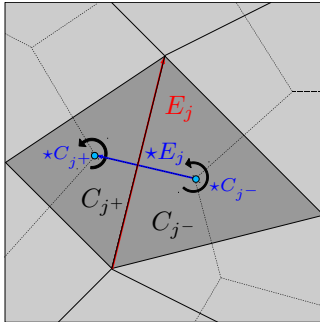


Figure 2: *Cell Complex*. The cell complex consists of cells  $C_i$  and oriented edges  $E_j$ , as well as the dual nodes  $*C_i$  and the dual edges  $*E_j$ . An edge  $E_j$  is the boundary between two cells, denoted by  $C_{j\pm}$ . Its dual  $*E_j$  connects the corresponding dual nodes.

Again we present the approach for two dimensional surfaces in  $\mathbb{R}^3$ . The simpler case of curves in  $\mathbb{R}^2$  is treated by analogy. We assume that the surface  $\Gamma$  is approximated by a polygonal surface  $\Gamma_C$  which consists of  $N_C$  planar *cells*,  $\{C_1, \dots, C_{N_C}\}$ , in the sense that the vertices of the cells lie on  $\Gamma$  and furthermore there exists a (bijective) projection  $\Pi_\Gamma : \Gamma_C \rightarrow \Gamma$  so that the images of the cells  $\Pi_\Gamma(C_i)$  form a partition of  $\Gamma$ . See Lenz, Némajieu and Rumpf[28] for a detailed discussion of such an approximation. The (oriented) boundaries  $\partial C_i$  are algebraic sums of  $N_E$  oriented *edges*  $\{E_1, \dots, E_{N_E}\}$ , so that every edge  $E_j$  is exactly the interface between two adjacent cells  $C_{j+}, C_{j-}$  oriented so that

$\pm E_j$  is part of  $\partial C_{j\pm}$  (fig.2). We denote by  $\partial_C$  the sparse  $N_E \times N_C$  matrix with non-zero elements  $(\partial_C)_{j,j\pm} = \pm 1$ . The metric-dependent information of the discretization is captured by the matrices  $|C| := \text{diag}(|C_1|, \dots, |C_{N_C}|)$  and  $|E| := \text{diag}(|E_1|, \dots, |E_{N_E}|)$ .

Furthermore, we assume that for every cell  $C_i$  there is an appropriately defined *dual node*  $\star C_i \in C_i$ . Based on this, we define for every edge  $E_j$  a dual edge connecting  $\star C_{j-}$  to  $\star C_{j+}$  with *dual edge length*  $|\star E_j| := \text{dist}(\star C_{j+}, \star C_{j-})$  gathered in the corresponding diagonal matrix  $|\star E| := \text{diag}(|\star E_1|, \dots, |\star E_{N_E}|)$ . Here  $\text{dist}(\cdot, \cdot)$  is the distance on  $\Gamma_C$ . An important case is when the cells  $C_i$  are the *Voronoi cells* of their dual nodes  $\star C_i$ .

Now, we approximate scalar quantities  $u$  over  $\Gamma$  with the vector  $u_C = (u_{C_i})_{i=1, \dots, n_C} \in \mathbb{R}^{N_C}$  of their mean value over the (projected) cells, so that

$$u_{C_i} \approx |\Pi_\Gamma(C_i)|^{-1} \int_{\Pi_\Gamma(C_i)} u \, da.$$

Likewise we approximate vector quantities  $v$  in the tangent bundle  $T\Gamma$  with the vector  $v_E = (v_{E_j})_{j=1, \dots, n_E} \in \mathbb{R}^{N_E}$  of their mean flux through the (projected) edges, so that

$$v_{E_j} \approx |\Pi_\Gamma(E_j)|^{-1} \int_{\Pi_\Gamma(E_j)} \langle v, \nu_j \rangle_\Gamma \, dl,$$

where  $\nu_j$  is the unit covector of  $\Pi_\Gamma(E_j)$  pointing into  $\Pi_\Gamma(C_{j+})$ .

Next, we introduce the following discrete differential operators  $\partial_{\text{grad}}$  and  $\partial_{\text{div}}$  as matrices in  $\mathbb{R}^{N_E, N_C}$  and  $\mathbb{R}^{N_C, N_E}$  with the aim of approximating  $\text{grad}_\Gamma$  and  $\text{div}_\Gamma$ , respectively. They are defined by

$$\partial_{\text{grad}} := |\star E|^{-1} \partial_C, \quad (21)$$

$$\partial_{\text{div}} := -|C|^{-1} \partial_C^T |E|. \quad (22)$$

where  $\partial_C$  is the matrix in  $\mathbb{R}^{N_E, N_C}$  with the non zero entries  $(\partial_C)_{j(j\pm)} = \pm 1$ , such that  $\partial_C u_C := (u_{C_{j+}} - u_{C_{j-}})_{j=1, \dots, N_E}$ . We also define the inner products

$$\langle u_C, \tilde{u}_C \rangle_C := u_C^T |C| \tilde{u}_C, \quad (23)$$

$$\langle v_E, \tilde{v}_E \rangle_E := v_E^T |\star E| |E| \tilde{v}_E \quad (24)$$

with associated norms  $|u_C|_C$  and  $|u_E|_E$ , respectively, so that  $\langle u_C, \tilde{u}_C \rangle_C \approx \int_\Gamma u \tilde{u} \, da$  and  $\langle v_E, \tilde{v}_E \rangle_E \approx \int_\Gamma \langle v, \tilde{v} \rangle_\Gamma \, da$ . Based on the fact that  $\partial_{\text{div}}^T |C| = -|E| |\star E| \partial_{\text{grad}}$  we deduce a discrete *integration by parts* property

$$\langle u_C, \partial_{\text{div}} v_E \rangle_C + \langle \partial_{\text{grad}} u_C, v_E \rangle_E = 0. \quad (25)$$

### 3.3 Discrete energy

Now, we are in the position to discretize our variational model in a straightforward way. Indeed, we define the discrete energy functional

$$\mathbf{E}(u_C) := \langle u_C, \zeta z_C - H_C \rangle_C + \frac{\epsilon}{2} \langle u_C, [\zeta \cos \theta_C - T_C] u_C \rangle_C + \frac{\epsilon}{2} |\partial_{\text{grad}} u_C|_E^2$$

on a vector  $u_C$  representing the discrete mass distribution in terms of fluid volume per unit surface. Here,  $\cos \theta_C$  is the vector of vertical component of the unit normal  $n$  on the cells,  $z_C$  the vector of vertical components of the dual vertices  $\star C_i$ ,  $T_C$  is the vector of discrete total curvature associated with the cells and defined by  $T_{C_i} = T(\Pi_\Gamma(\star C_i))$ . We have also used the notation  $[v] := \text{diag}(v_1, \dots, v_n)$ , to denote the diagonal matrix with the elements of the vector  $v$  in the diagonal. Using (25), it can be put in the general quadratic form

$$\mathbf{E}(u_C) = \langle \alpha_C, u_C \rangle_C + \frac{\epsilon}{2} \langle B u_C, u_C \rangle_C \quad (26)$$

where

$$\alpha_C = \zeta z_C - H_C, \quad (27a)$$

$$B = [\zeta \cos \theta_C - T_C] - \partial_{\text{div}} \partial_{\text{grad}}. \quad (27b)$$

### 3.4 Discrete dissipation and mobility

The discrete metric takes the form

$$\mathbf{g}_{u_C}(f_E, f_E) := \langle f_E, [\mathbf{M}_E(u_C)] f_E \rangle_E, \quad (28)$$

where the discrete mobility  $\mathbf{M}_E(u_C) \in \mathbb{R}^{N_E}$  is a vector, which attaches a mobility value  $\mathbf{M}_E(u_C)_j$  to every edge  $E_j$ . To derive a suitable discrete mobility we first define a scalar mobility  $\mathbf{M}_{E_j}(u) := \frac{1}{3}u^3 + \frac{\epsilon}{6}u^4(H_{E_j} + \kappa_{E_j})$  at every edge, which is associated with fluxes in normal direction across the edge. Here,  $H_{E_j}$  denotes the mean curvature of  $\Gamma$  evaluated at the projection  $\Pi_\Gamma x_{E_j}$  of the center of mass  $x_{E_j}$  on the edge  $E_j$  and  $\kappa_{E_j} := \langle \nu_j, S_{E_j} \nu_j \rangle_\Gamma$  is the normal curvature in the direction of the conormal  $\nu_j$  on the projected edge  $\Pi_\Gamma(E_j)$  with  $S_{E_j}$  being the shape operator at  $\Pi_\Gamma x_{E_j}$ . Following Grün and Rumpf[21] we now choose  $\mathbf{M}_E(u_C)$  as the integral harmonic mean

$$\mathbf{M}_E(u_C) := \left( \frac{1}{u_{C_{j+}} - u_{C_{j-}}} \int_{u_{C_{j-}}}^{u_{C_{j+}}} M_{E_j}(t) dt \right)^{-1} \quad (29)$$

with the convention  $\mathbf{M}_E(u_C) = M_{E_j}(u_{C_{j+}})$  if  $u_{C_{j+}} = u_{C_{j-}}$ . To motivate this choice, let us consider the planar surface case, where one defines an entropy function  $G$  as the second root of the inverse of the scalar mobility  $M$ , i. e.  $G(u) := \int_0^u \int_0^s \frac{1}{M(t)} dt ds$ . Then,  $G''(u) = M(u)^{-1}$  implies that  $M(u) \text{grad } G'(u) = \text{grad } u$  and based on this observation an a priori estimate for the integral of the entropy function can be deduced (cf. Beretta, Bertsch and Dal Paso[3]). Thus, in the flat case or on a sphere our choice for the discrete mobility allows to mimic this equality. In fact, the entries of  $\mathbf{M}_E(u_C)$  no longer depend on varying curvature quantities attached to edges and we immediately obtain that  $\mathbf{M}_E(u_C) := [\partial_C \mathbf{G}'_E(u_C)]^{-1} \partial_C u_C$  for the associated  $\mathbf{G}_E(u) := \int_0^u \int_0^s \frac{1}{M_E(t)} dt ds$  and thus  $[\mathbf{M}_E(u_C)] \partial_{\text{grad}} \mathbf{G}'_E(u_C) = \partial_{\text{grad}} u_C$ . In the case of a flat surface and for the mobility been implicitly evaluated at the new time step, one can derive from

this equality an a priori bound for the vector  $\mathbf{G}(u_{C_j})_{j=1,\dots,n}$  of entropy values on the cells (cf. Grün, Lenz and Rumpf[22]). This allows one to prove that the strict positivity of  $u_C$  is maintained during the evolution. Unfortunately, this proof can not be extended in a straightforward manner to the curved case, because of the added effects of the geometry of the substrate on the evolution of the thin film. In practice, we experimentally observe that the numerical solution remains indeed positive even with very thin precursor layers (cf. §5). We intend to deal with the issue of positivity in future work, by considering more general models which involve the Navier slip condition and certain van der Waals-like forces. These extensions tend to promote the preservation of positivity for the thickness of the thin film during its evolution (cf. §V in Craster and Matar[10]).

### 3.5 Discrete conservation law

In analogy to the continuous case the discrete metric  $\mathbf{g}$  is defined in terms of the discrete flux  $f_E$  whereas the discrete energy  $\mathbf{E}$  is evaluated on the discrete mass distribution  $u_C$ . In the continuous case, the flux  $f$  and the mass distribution quantity  $u$  are coupled via the transport equation  $\dot{u} + \text{div}_\Gamma(M(u)f) = 0$ . Now, we discretize this transport process to couple  $f_E$  and  $u_C$  using the DEC approach. Given, the vector  $u_C^k$  as an approximation of  $u$  at time  $t^k$  we consider the linear system of equations

$$u_C - u_C^k + \tau \partial_{\text{div}} [\mathbf{M}_E(u_C^k)] f_E = 0 \quad (30)$$

where  $\tau$  is the time step size. Here,  $u_C$  and  $f_E$  are considered as approximations of  $u(t^{k+1})$  at time  $t^{k+1} = t^k + \tau$  and  $f|_{[t^k, t^{k+1}]}$ , respectively.

### 3.6 Fully discrete natural time discretization

Finally, using (26), (28), and (30) we derive the also spatially discrete counterpart of the time discretization (20) and obtain the following fully discrete variational time discretization for thin film flow on a polygonal surface  $\Gamma_C$ : Given  $u_C^k \in \mathbb{R}^{N_C}$  at time  $t^k$  find  $(u_C^{k+1}, f_E^{k+1}) \in \mathbb{R}^{N_C} \times \mathbb{R}^{N_E}$  at time  $t^{k+1} = t^k + \tau$  as the solution of the following constraint optimization on  $\mathbb{R}^{N_C} \times \mathbb{R}^{N_E}$ :

$$\min_{u_C, f_E} \left\{ \frac{\tau}{2} \mathbf{g}_{u_C^k}(f_E, f_E) + \mathbf{E}[u_C] \right\}, \quad (31a)$$

$$\text{where } u_C - u_C^k + \tau \partial_{\text{div}} [\mathbf{M}_E(u_C^k)] f_E = 0. \quad (31b)$$

Furthermore, for the functional to be minimized we get

$$\frac{\tau}{2} \mathbf{g}_{u_C^k}(f_E, f_E) + \mathbf{E}[u_C] = \frac{\tau}{2} \langle f_E, \mathbf{M} f_E \rangle_E + \langle u_C, \alpha_C \rangle_C + \frac{\epsilon}{2} \langle u_C, B u_C \rangle_C. \quad (32)$$

with  $\mathbf{M} := [M(u_C^k)]$ . Thus we are lead to a *equality-constrained quadratic programming* problem. The  $N_E \times N_E$  diagonal matrix  $\mathbf{M}$  is positive definite under the assumption that  $u_C^k > 0$ . The second term of the  $N_C \times N_C$  matrix  $B$ , namely the matrix  $-\partial_{\text{div}} \partial_{\text{grad}}$ , is symmetric and positive semidefinite with respect to

the scalar product  $\langle \cdot, \cdot \rangle_C$ , i.e.  $\langle x_C, -\partial_{\text{div}} \partial_{\text{grad}} y_C \rangle_C = \langle \partial_{\text{grad}} x_C, \partial_{\text{grad}} y_C \rangle_E = \langle -\partial_{\text{div}} \partial_{\text{grad}} x_C, y_C \rangle_C$  and  $\langle x_C, -\partial_{\text{div}} \partial_{\text{grad}} x_C \rangle_C = \langle \partial_{\text{grad}} x_C, \partial_{\text{grad}} x_C \rangle_E \geq 0$ . The matrix  $B$  itself is also symmetric wrt  $\langle \cdot, \cdot \rangle_C$  but in general not positive semidefinite due to the diagonal term  $\zeta \cos \theta_C - T_C$ , which might be negative on curved geometries or in the presence of gravity, more specifically when the film is located underneath the substrate (cf. Lister *et al.*[29]).

## 4 Solving the Optimization Problem

Instead of solving the constrained optimization problem (31) directly, we can reduce it to a more convenient form by using the constraint to eliminate  $u_C$ . First, we substitute  $u_C$  with  $u_C^k + \delta u_C$ , where  $\delta u_C := u_C - u_C^k$ , to get

$$\min_{f_E} \left\{ \frac{\tau}{2} \langle f_E, \mathbf{M} f_E \rangle_E + \frac{\epsilon}{2} \langle \delta u_C, B \delta u_C \rangle_C + \langle \delta u_C, \alpha_C + \epsilon B u_C^k \rangle_C + R[u_C^k] \right\} \quad (33)$$

with  $\delta u_C = \delta u_C(f_E) = -\tau \partial_{\text{div}} \mathbf{M} f_E$  and  $R[u_C^k] := \frac{\epsilon}{2} \langle u_C^k, B u_C^k \rangle_C + \langle u_C^k, \alpha_C \rangle_C$  being independent of  $f_E$  and  $\delta u_C$ . Finally, eliminating  $\delta u_C$  we achieve the unconstrained optimization problem:

$$\min_{f_E} \left\{ \frac{1}{2} \langle f_E, A f_E \rangle_E + \langle f_E, b_E \rangle_E \right\}$$

where  $A = \tau \mathbf{M} - \epsilon \tau^2 \mathbf{M} \partial_{\text{grad}} B \partial_{\text{div}} \mathbf{M}$  and  $b_E = \tau \mathbf{M} \partial_{\text{grad}} (\alpha_C + \epsilon B u_C^k)$ . For a solution to exist and be unique, the matrix  $A$  needs to be positive definite with respect to the inner product  $\langle \cdot, \cdot \rangle_E$ .

**Positive definiteness of  $A$ .** In this section, we use ideas from convex optimization theory to derive a sufficient condition for the time step  $\tau$  for  $A$  to be positive definite. We recall that  $A = \tau \mathbf{M} - \epsilon \tau^2 \mathbf{M} \partial_{\text{grad}} B \partial_{\text{div}} \mathbf{M}$ , where  $B = [R_C] - \partial_{\text{div}} \partial_{\text{grad}}$  with  $R_C := \zeta \cos \theta_C - T_C$ , and we let  $\underline{R}$  be the minimum entry of  $R_C$  and  $\sigma(\mathbf{M})$  the spectral radius of  $\mathbf{M}$ . We define  $\tau_{\max} := \frac{4}{\epsilon \underline{R}^2 \sigma(\mathbf{M})}$  if  $\underline{R} < 0$ , and  $\tau_{\max} := \infty$  otherwise. In what follows we will show that  $\tau_{\max}$  is indeed an upper bound for the time step, which guarantees positive definiteness of the matrix  $A$ , i. e.

$$0 < \tau < \tau_{\max} \Rightarrow A \text{ pos. definite wrt } \langle \cdot, \cdot \rangle_E. \quad (34)$$

Let us emphasize that  $\tau_{\max}$  only depends on the physical configuration and not on the spatial grid size. By definition of  $A$  and (32) we have

$$\begin{aligned} \langle f_E, A f_E \rangle_E &= \tau \langle f_E, \mathbf{M} f_E \rangle_E + \epsilon \langle \delta u_C, B \delta u_C \rangle_C \\ &= \tau \langle f_E, \mathbf{M} f_E \rangle_E + \epsilon \langle \delta u_C, [R_C] \delta u_C \rangle_C + \epsilon |\partial_{\text{grad}} \delta u_C|_E^2 \end{aligned} \quad (35)$$

for any  $f_E \in \mathbb{R}^{N_E}$  and  $\delta u_C = -\tau \partial_{\text{div}} \mathbf{M} f_E$ . If  $\underline{R} \geq 0$  then  $B = [R_C] - \partial_{\text{div}} \partial_{\text{grad}}$  is positive semidefinite and together with the positive definiteness of  $\mathbf{M}$  we indeed obtain that  $A$  is positive definite for any  $\tau > 0$ . If  $\underline{R} < 0$ , then given that

$-\epsilon \langle \delta u_C, [R_C] \delta u_C \rangle_C \leq \epsilon |\underline{R}| |\delta u_C|_C^2$ , it is sufficient to ensure that the matrix  $\underline{A}$  defined by

$$\langle f_E, \underline{A} f_E \rangle_E := \tau \langle f_E, \mathbf{M} f_E \rangle_E - \epsilon |\underline{R}| |\delta u_C|_C^2 + \epsilon |\partial_{\text{grad}} \delta u_C|_E^2 \quad (36)$$

is positive definite provided the condition  $0 < \tau < \tau_{\max} = \frac{4}{\epsilon \underline{R}^2 \sigma(\mathbf{M})}$  holds. To this end we first verify the inequality

$$\alpha |\delta u_C|_C^2 \leq \frac{\tau}{2} \langle f_E, \mathbf{M} f_E \rangle_E + \frac{\tau \alpha^2 \overline{\mathbf{M}}}{2} |\partial_{\text{grad}} \delta u_C|_E^2 \quad (37)$$

for any  $\alpha > 0$ . Let  $F_{\delta u_C}$  denote the set of  $f_E$  which satisfy this transport equation for a specific  $\delta u_C$ . The dissipation associated with  $\delta u_C$  is then given by the constrained minimization problem  $\min_{f_E \in F_{\delta u_C}} \frac{\tau}{2} \langle f_E, \mathbf{M} f_E \rangle_E$ . We denote the objective function  $\frac{\tau}{2} \langle f_E, \mathbf{M} f_E \rangle_E$  with  $\mathcal{D}(f)$ . This is a constrained optimization problem, so we may consider its dual problem (see Chapter 5 in Boyd and Vandenberghe[8]). We write down the Lagrange function, with Lagrange multiplier  $p_C \in \mathbb{R}^{N_C}$ :

$$\begin{aligned} \mathcal{L}(f_E, p_C) &= \mathcal{D}(f) - \langle p_C, \delta u_C + \tau \partial_{\text{div}} \mathbf{M} f_E \rangle_C \\ &= \frac{\tau}{2} \langle f_E, \mathbf{M} f_E \rangle_E + \tau \langle \partial_{\text{grad}} p_C, \mathbf{M} f_E \rangle_E - \langle p_C, \delta u_C \rangle_C \end{aligned}$$

For a fixed  $p_C$ ,  $\mathcal{L}(\cdot, p_C)$  is strictly convex, and the unique minimum is achieved at  $f_E = -\partial_{\text{grad}} p_C$ . The dual Lagrange function then is then

$$\begin{aligned} \mathcal{L}^*(p_C) &:= \inf_{f_E} \mathcal{L}(f_E, p_C) = \mathcal{L}(-\partial_{\text{grad}} p_C, p_C) \\ &= -\frac{\tau}{2} \langle \partial_{\text{grad}} p_C, \mathbf{M} \partial_{\text{grad}} p_C \rangle_E - \langle p_C, \delta u_C \rangle_C. \end{aligned}$$

For any  $p_C$  and any  $f_E$  we obtain by the *duality* inequality  $\mathcal{L}^*(p_C) \leq \mathcal{D}(f_E)$  the estimate  $-\frac{\tau}{2} \langle \partial_{\text{grad}} p_C, \mathbf{M} \partial_{\text{grad}} p_C \rangle_E - \langle p_C, \delta u_C \rangle_C \leq \frac{\tau}{2} \langle f_E, \mathbf{M} f_E \rangle_E$ . Finally, choosing  $p_C = -\alpha \delta u_C$ , for an arbitrary  $\alpha > 0$ , we obtain

$$\begin{aligned} \alpha |\delta u_C|_C^2 &\leq \frac{\tau}{2} \langle f_E, \mathbf{M} f_E \rangle_E + \frac{\tau \alpha^2}{2} \langle \partial_{\text{grad}} \delta u_C, \mathbf{M} \partial_{\text{grad}} \delta u_C \rangle_E \\ &\leq \frac{\tau}{2} \langle f_E, \mathbf{M} f_E \rangle_E + \frac{\tau \alpha^2 \sigma(\mathbf{M})}{2} |\partial_{\text{grad}} \delta u_C|_E^2, \end{aligned}$$

which is the required estimate (37).

Next, we assuming that  $\tau < \frac{4}{\epsilon \underline{R}^2 \sigma(\mathbf{M})}$  and setting  $\alpha = \frac{\epsilon |\underline{R}|}{2}$  in inequality (37) and obtain

$$\begin{aligned} \epsilon |\underline{R}| |\delta u_C|_C^2 &\leq \tau \langle f_E, \mathbf{M} f_E \rangle_E + \frac{\tau \epsilon^2 \underline{R}^2 \sigma(\mathbf{M})}{4} |\partial_{\text{grad}} \delta u_C|_E^2 \\ &\leq \tau \langle f_E, \mathbf{M} f_E \rangle_E + \epsilon |\partial_{\text{grad}} \delta u_C|_E^2. \end{aligned} \quad (38)$$

Hence,  $\underline{A}$  is positive semidefinite. Now, assume that

$$0 = \langle f_E, \underline{A} f_E \rangle_E = \tau \langle f_E, \mathbf{M} f_E \rangle_E - \epsilon |\underline{R}| |\delta u_C|_C^2 + \epsilon |\partial_{\text{grad}} \delta u_C|_E^2 \quad (39)$$

Revisiting inequality (38), we observe that for  $\partial_{\text{grad}}\delta u_C \neq 0$  the sharper inequality  $\epsilon|\underline{R}|\delta u_C|_C^2 < \tau\langle f_E, \mathbf{M}f_E \rangle_E + \epsilon|\partial_{\text{grad}}\delta u_C|_E^2$  is obtained. This implies  $\langle f_E, \underline{A}f_E \rangle_E > 0$  and leads to a contradiction. Thus, we already know that  $\partial_{\text{grad}}\delta u_C = 0$ . Furthermore, we deduce from the fact that (37) holds for all  $\alpha > 0$  that  $\delta u_C = 0$  and then from (39) that  $0 = \langle f_E, \mathbf{M}f_E \rangle_E$ . By the positive definiteness of  $\mathbf{M}$  we finally achieve  $f_E = 0$ . Hence, we have verified that  $\underline{A}$  and consequently  $A$  are positive definite.

## 5 Experimental Convergence Analysis

Before we apply the presented approach to physically interesting scenarios of thin film flow on curves or surfaces let us investigate the robustness and accuracy of the underlying variational time step discretization and the spatial discretization based on discrete exterior calculus experimentally. Let us once more emphasize that we assume strictly positive film height and hence do not treat the propagation of triple lines formed by the solid, liquid, gas interfaces. Nevertheless, we will consider transport and spreading of films with very small film height.

At first we consider the evolution of thin films on 1D substrates. In Figures 3 - 6, we present certain experimental numerical convergence tests of the proposed scheme. Here, the underlying thickness parameter is  $\epsilon = 0.01$  for a domain of diameter in the horizontal direction  $\approx 1$ . In Fig. 3, a Gaussian droplet with (rescaled) height 1 put on top of a uniform layer with thickness 0.1 is flowing down a curved substrate ( $\zeta = 5$ ). To test convergence in space, we evolved the initial condition for a small time on spatial grids of various resolutions (32 through 65536 nodes) and compared the discrete solution with the discrete solution at the finest grid in the discrete  $L^2$  norm  $\|\cdot\|_C$ . Here, the time step size is considered to be very small, i.e. we chose  $\tau = 1.526 \times 10^{-5}$ . To test convergence in time, we evolve the same initial film profile on a grid with 1024 nodes for a fixed time interval, but for various values of  $\tau$ . We calculate solutions for  $\tau = T$  through  $\tau = T/2048$  (with  $T = 4$ ) and compare with the solution obtained for the finest time step size. Both in time and space we observe linear numerical convergence rates as plotted in Figure 3. In Fig.4, we run the same evaluations for a parabolic droplet on top of a uniform layer with thickness 0.01 under stronger gravity ( $\zeta = 50$ ). Although our model can not handle partially wetted surfaces, this configuration with a discontinuous derivative at the edge of the initial droplet together with a very thin precursor layer exhibits a similar behavior. For sufficiently small time step  $\tau$  we experimentally observe a linear convergence rate with respect to  $\tau$ . Furthermore, tracking the position  $X_{\text{triple}}(t)$  of the advancing front of the droplet (the approximate "triple point") illuminates why the time step needs to be controlled; although the method is stable even for large  $\tau$ , the front can only advance one cell per time step and hence a CFL-type condition  $\tau V \leq h$ , with  $V$  being the speed of the front, must be met. Once this is fulfilled, our results show that the trajectory  $X_{\text{triple}}$  converges linearly with respect to  $\tau$ .

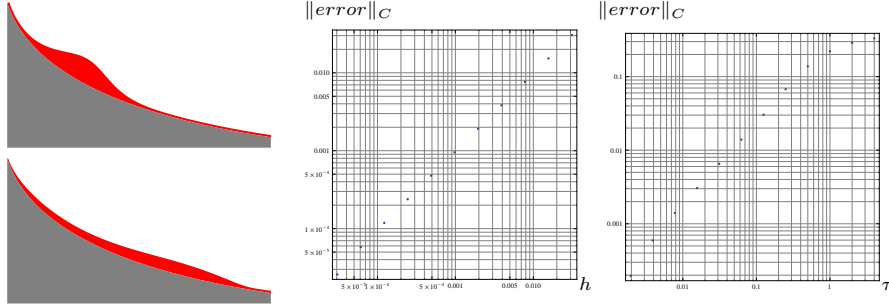


Figure 3: A Gaussian droplet with a preset precursor layer evolves on an inclined curved substrate, where the initial [Left Top] and the final [Left Bottom] state are displayed. Furthermore, a Log-plot of the  $L^2$ -norm of the error for varying grid size  $h$  [Middle] as well as for varying time step  $\tau$  [Right] is plotted.

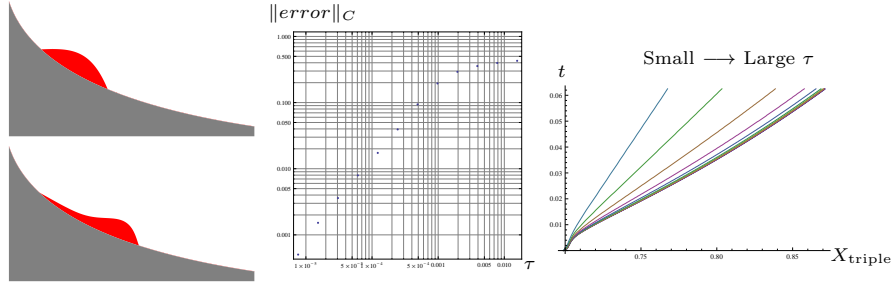


Figure 4: A parabolic droplet on an inclined curved substrate spreads on top of a thin precursor layer. Initial [Left Top] and final [Left Bottom] state are shown. Furthermore, we display [Middle] a Log-plot of the  $L^2$ -norm of the error for different values of the time step size  $\tau$  (for fixed spatial resolution  $h = 1.22 \times 10^{-4}$ ) and [Right] the evolution of the location  $X_{\text{triple}}(t)$  of the advancing droplet front is plotted for time step sizes  $\tau = \{0.0625h, 0.125h, 0.25h, 0.5h, h, 2h, 4h, 8h, 16h\}$ .

Next, in Figures 5 and 6 we study the merging of two droplets on a concave substrate and the splitting of a uniform layer on a convex substrate, respectively. For the merging droplets, we consider two Gaussian droplets with height 1 on a precursor layer with thickness 0.1 on a concave (parabolic) substrate. The configuration is symmetric and both gravity ( $\zeta = 1$ ) and curvature pull the droplets into the sink and downwards on both sides, respectively. Plotting the value of  $u$  at the contact point as a function of time reveals a non-monotone behavior in Figure 5; as the droplets come in contact the thickness of the thin film between them initially decreases, similar to the effect of a capillary ridge. In Fig.6 we take into account as initial configuration a uniform layer of thickness 0.5 on a convex (parabolic) substrate with grid resolution  $h = 2 \times 10^{-3}$  with no gravity ( $\zeta = 0$ ). Surface tension drives the fluid away from the region of largest negative curvature at the tip of the substrate. Plotting the graph of minimum  $u$

versus time reveals a rapid initial decrease of  $u$  until it is approximately 10% of the initial value and then the evolution slows down significantly as the mobility  $M(u)$  becomes small.

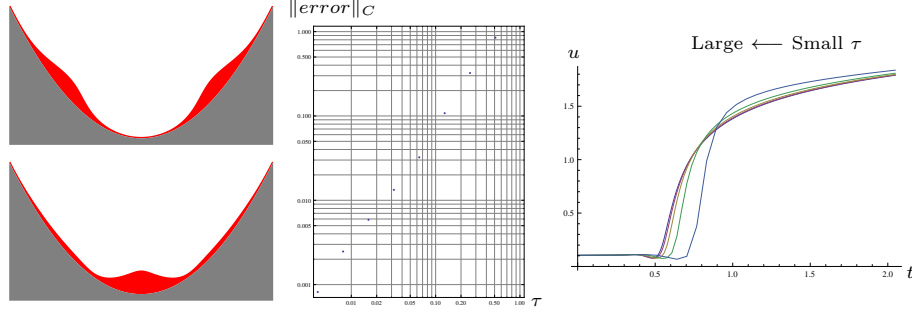


Figure 5: For two merging droplets the initial [*Left Top*] and the final [*Left Bottom*] configuration are shown. Again, we plot on a logarithmic scale the  $L^2$ -norm of the error for varying time step  $\tau$  and fixed spatial resolution  $h = 5 \times 10^{-4}$  [*Middle*]. Furthermore, the evolution of  $u$  at the lowest point of the substrate (where the droplets collide) is shown, for time step sizes  $\tau = \{8h, 16h, 32h, 64h, 128h\}$  [*Right*].

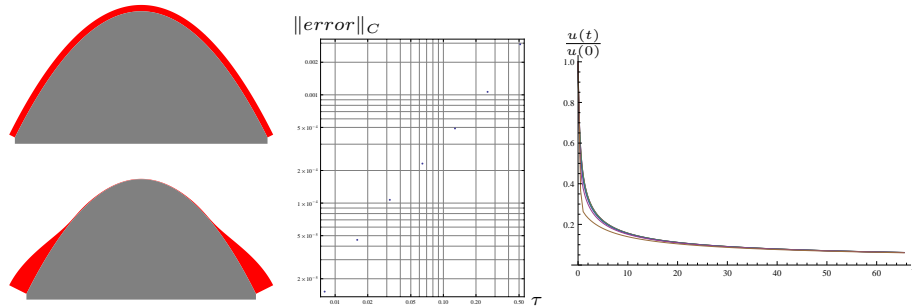


Figure 6: A uniform initial layer [*Left Top*] evolves towards a configuration [*Left Bottom*] with a partially (almost) dewetted area in the regions of largest negative curvature. The Log-plot of the  $L^2$ -norm of the error for varying time step  $\tau$  fixed spatial resolution  $h = 2 \times 10^{-3}$  is shown [*Middle*]. Finally, the evolution of  $u$  at the highest point of the substrate is plotted in time for time step sizes  $\tau = \{4h, 8h, 16h, 32h, 64h, 128h, 256h\}$  [*Right*].

In Fig. 7, we present numerical tests for the proposed method on a 2D substrate. The values of the parameters are  $\epsilon = 0.01$  and  $\zeta = 10$ . The substrate is a parametric surface of the form  $(\phi, r \cos(\theta(\phi)), r \sin(\theta(\phi))) \in \mathbb{R}^3$  with  $\theta(\phi) = \frac{\pi}{32}(\cos(\phi) - 1)$ , for  $(\phi, r) \in [0, 2\pi] \times [0, 8]$ . The initial condition is a Gaussian of unit height on a uniform layer of thickness 0.1. We follow the same procedure for the numerical convergence tests as in the 1D case. The tests for space convergence are performed on a sequence of regular  $2^m \times 2^m$  grids for  $m = 4 \dots 10$  for a fixed time step  $\tau = 10^{-4}$ . The convergence tests with respect to the time

step size are performed on a  $512 \times 512$  grid for values of  $\tau$  from  $\tau = T$  down to  $\tau = T/256$ . In both cases we observe numerical convergence in the discrete  $L^2$ -norm once a CFL-type condition is met, like in the 1D case.

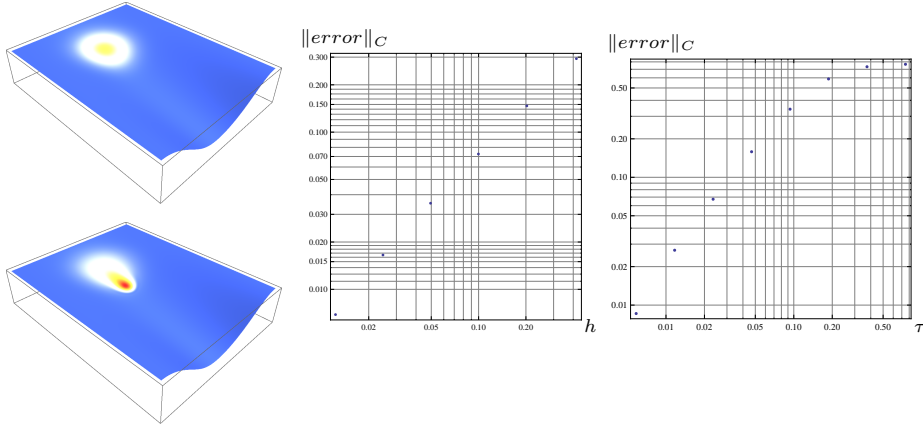


Figure 7: A Gaussian droplet [Left Top] evolves on an inclined curved substrate with precursor layer (intermediate film profile [Bottom Left]). The mass density  $u$  is color-coded as . Again a Log-plot of the  $L^2$ -norm of the error versus the grid size  $h$  for fixed time step size  $\tau = 10^{-4}$  [Middle] and versus the time step size  $\tau$  for fixed grid size  $h = 1.23 \times 10^{-2}$  [Right].

## 6 Numerical Simulation

### 6.1 1D droplet on a slide

In Figures 8 and 9, we study the evolution of a droplet sliding down a 1D inclined cascade of sinks, where the substrate shape is a cosine curve rotated clockwise by  $\frac{\pi}{5}$ . The initial condition is a Gaussian of height 15 on top of a precursor layer of thickness 0.01 and the underlying parameters are  $\epsilon = 0.1$  and  $\zeta = 1$ . The curved is discretized with 1000 nodes ( $h = 0.031$ ) and the time step is  $\tau = h/10$ .

The evolution of the film is driven by the gradient of the energy, with the physical meaning of a pressure  $P = (\zeta z - H) + \epsilon(\zeta \cos \theta - T)u - \epsilon \Delta_{\Gamma} u$ . The leading order term  $P_0 = \zeta z - H$ , which is independent of  $u$ , tends to pull the film towards its local minima (cf. the validation examples in Section 5). The concentration of fluid in a sink around a local minimum of  $(\zeta z - H)$  of the substrate graph increases the term  $-\epsilon \Delta u$  which tends to make the minimum more "shallow". Once enough fluid is available in a single sink during the evolution, the pressure becomes almost flat around the minimum, i.e. the fluid is locally near a state of equilibrium. If even more fluid becomes available, it will

”spill over” potentially to a different, previously non accessible, local minimum of  $P_0$ . Thus, in the evolution the fluid fills a succession of ”reservoirs” as it flows down the substrate. The approximate contact point moves down the cascade and is characterized by a negative spike in the pressure.

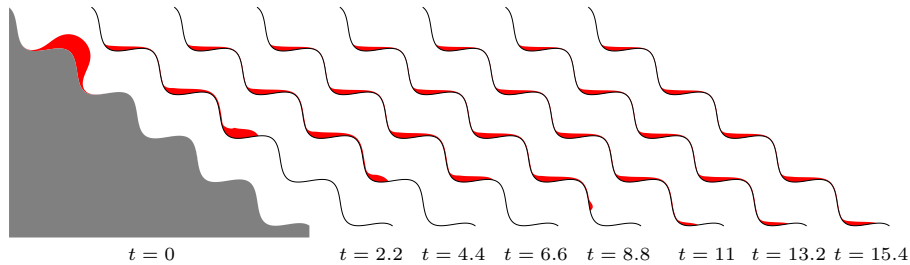


Figure 8: Evolution of a thin film on the inclined cascade of sinks.

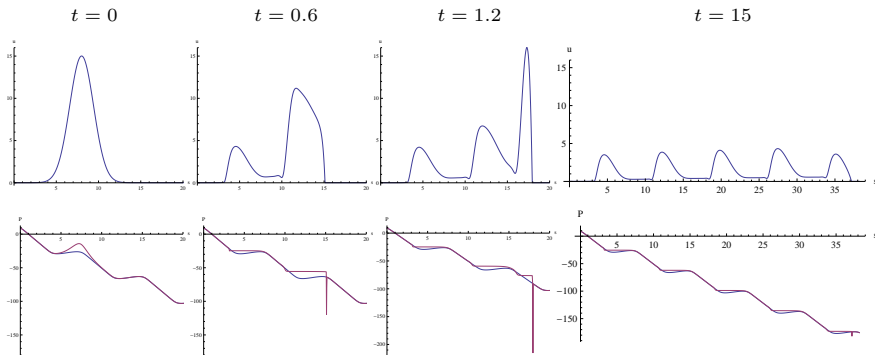


Figure 9: Plot of the mass concentration  $u$  [Top Row] and the corresponding pressure (overlaid on the leading order pressure term) [Bottom Row] for the evolving thin film on the inclined substrate at different times.

## 6.2 Film evolution in rotationally symmetric cavity

In Figures 11 and 12, we study the evolution of a uniform initial layer on a concave surface of revolution, similar to a *pulmonary alveolus*. The initial thickness is  $u(0) = 0.01$  and the parameters of the simulation are  $\epsilon = 0.01$  and  $\zeta = 0$ , i.e. there is no gravity (on a geometric microscale the effect of gravity can be neglected). Due to the rotational symmetry of the problem, we can reduce it to a 1D problem on the profile curve whose rotation generates the surface. Energy and dissipation are adapted taking into account the local radius parameter  $r$ . As explained in the previous section, the fluid tends to flow away from the minima of the mean curvature  $H$ , where the pressure  $P = -H + O(\epsilon)$  is high, and

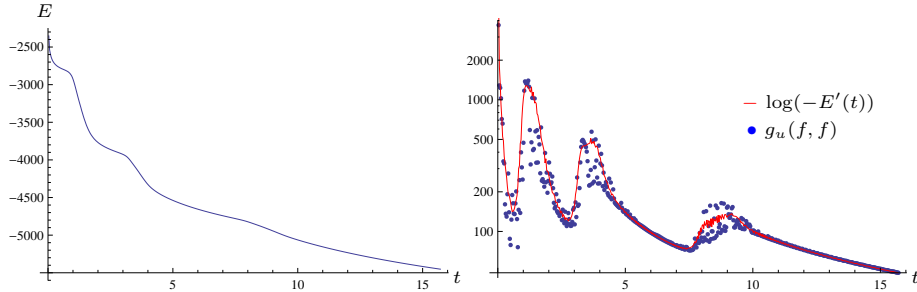


Figure 10: The graph of the energy  $E(u(t))$  [Left] and the logarithm of the negative rate of change of the energy  $E'(t)$  (solid line) overlaid with dots representing the dissipation rate  $g_u(f, f)$  plotted over time.

pool around its minima. The mean curvature of the surface of revolution is the sum of the two principal curvatures  $\kappa_1$  and  $\kappa_2$ . Let us denote by  $\kappa_1 = \frac{\sin \theta}{r}$  the curvature corresponding to the rotational circles, where  $\theta$  is the angle of  $n$  with the rotation axis, whereas the curvature  $\kappa_2$  is the curvature of the profile curve. If the problem was genuinely 1D, in which case  $H \equiv \kappa_2$ , the fluid would evacuate the neck of the cavity and pool over its apex. In the rotational symmetric 2D case, reflected by the impact of  $\kappa_1$ , there are local minima of  $-H$  in the neck region as well and part of the fluid will concentrate in a ring inside the neck of the cavity (fig. 11).

The long term behavior of the thin film can be understood by studying the pressure graph in fig. 12. Comparing the initial pressure with the pressure at a sufficiently advanced time, we observe that the fluid concentrates in droplets around the minima of  $-H$  and the pressure becomes locally almost constant, i.e. the fluid is locally close to equilibrium.

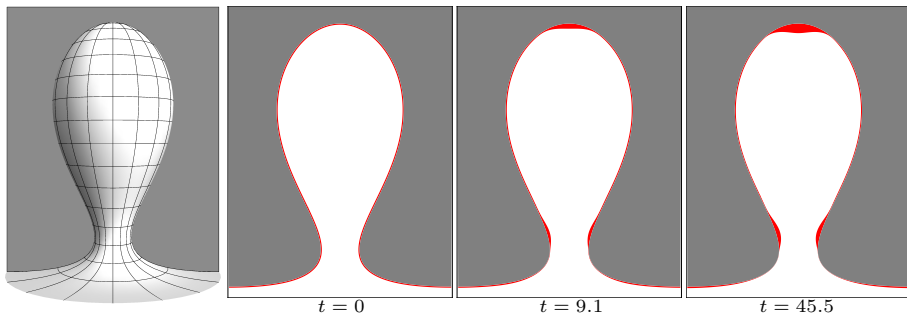


Figure 11: Different time steps of the evolution [Right] of the thin film inside a rotational symmetric cavity [Left] with a graph of the mass concentration and *not* the actual shape of the film in red.

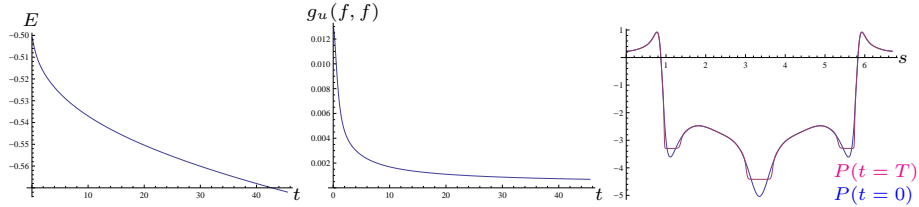


Figure 12: Graphs of the energy  $E[u]$  [Left], the dissipation  $g_u(f, f)$  [Middle] and a plot of the initial and final pressure [Right] over the arc-length of the curve.

### 6.3 Fingering flows

In Fig. 13 we present the evolution of a band of fluid flowing down an undu-

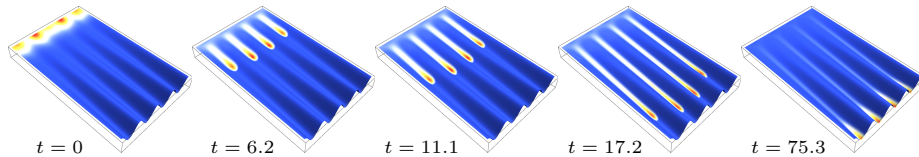


Figure 13: A band of fluid is separating and flowing downwards on inclined undulating surface. The evolution is shown at different times, with the mass concentration color-coded as .

lating surface. The values of the parameters are  $\epsilon = 0.05$  and  $\zeta = 20$ . The substrate is a parametric surface of the form  $(\phi, r \cos(\theta(\phi)), r \sin(\theta(\phi))) \in \mathbb{R}^3$  with  $\theta(\phi) = \frac{\pi}{64}(\cos(4\phi) - 1)$ , for  $(\phi, r) \in [0, 2\pi] \times [0, 8]$ . The initial condition is a Gaussian of unit height on a uniform layer of thickness 0.1. The spreading of the band exhibits the phenomenon of *fingering*, where droplets break away from the spreading front and larger droplets in the middle advance with higher velocity than smaller droplets on both sides. The separation, in this case, is driven by the shape of the substrate. For a related experimental study of fingering phenomena of thin films on a cylinder and sphere we refer to Takagi and Huppert[43], where the influence of the Bond number on the fingering instability is analyzed.

In Fig. 14 we show the evolution of a thin film on a sphere. The initial condition is a perturbed droplet on the north pole of the sphere, on top of a precursor layer with thickness  $u_{min} = 0.01$ . The discretized sphere has 25002 nodes and the model parameters are  $\epsilon = 0.01$  and  $\zeta = 10$ . The droplet spreads towards the equator but triggered by an initial perturbations fingering instabilities can be observed, this time caused by unstable nature of the flow itself (cf. Greer, Bertozzi and Shapiro[20]). For large enough times, the fluid pools under the south pole. For the numerical simulation of thin film flow on prolate spheroid, approximating the shape of the human cornea we refer to Braun *et al.*[9], where both Newtonian and non-Newtonian (shear thinning) fluids are investigated.

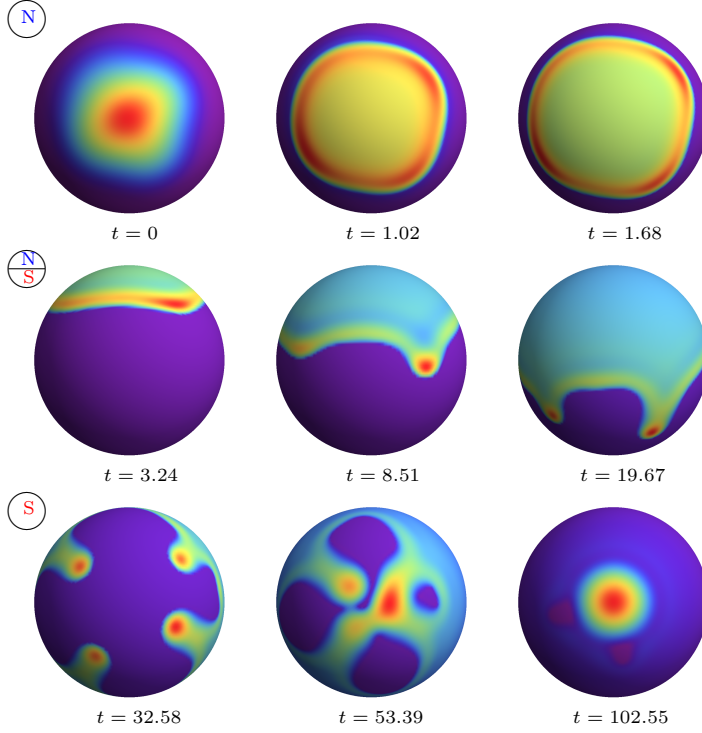


Figure 14: The fingering evolution of a droplet on a sphere is displayed at different times (north pole view [Top], equatorial view [Middle], south pole view [Bottom]). The mass concentration is color-coded as .

## A The Rate-of-strain Tensor.

Following the approach by Roy, Roberts and Simpson[39] and the discussion in Batchelor[2] (Appendix 2), we consider a parametrization  $x(\xi_1, \xi_2)$  of  $\Gamma$ , such that the corresponding coordinate system  $(\xi_1, \xi_2)$  is orthogonal and the coordinate lines are aligned with the principal directions of  $\Gamma$ . This coordinate system can be extended into an orthogonal coordinate system  $(\xi_1, \xi_2, \xi_3 \equiv \xi)$  on  $\mathcal{X}_{eh}(\Gamma) \subset \mathbb{R}^3$  using the mapping  $\phi$ :

$$\mathbf{x}(\xi_1, \xi_2, \xi_3) := \phi(x(\xi_1, \xi_2), \xi_3) = \phi_0(x(\xi_1, \xi_2)) + \epsilon \xi_3 n(x(\xi_1, \xi_2)).$$

We introduce scale factors  $h_i = \left| \frac{\partial \mathbf{x}}{\partial \xi_i} \right|$  for  $i = 1, 2, 3$ . Using the expression for  $d\phi$  from Section 2, we have  $\frac{\partial \mathbf{x}}{\partial \xi_\alpha} = d\phi(\Lambda \frac{\partial x}{\partial \xi_\alpha})$  and so  $h_\alpha = \lambda_\alpha \tilde{h}_\alpha = (1 - \epsilon \xi_3 \kappa_\alpha) \tilde{h}_\alpha$  for  $\alpha = 1, 2$ , where  $\kappa_\alpha$  are the principal curvatures of  $\Gamma$  and  $\tilde{h}_\alpha = \left| \frac{\partial x}{\partial \xi_i} \right|_\Gamma$  are the corresponding scale factors on  $\Gamma$ . For the normal direction, we have  $\frac{\partial \mathbf{x}}{\partial \xi_3} = \epsilon n$  and so  $h_3 = \epsilon$ . Now, consider the velocity field  $v$  in  $\mathcal{X}_{eh}(\Gamma)$ . Using the orthonormal basis  $(e_1, e_2, e_3 \equiv n)$  associated with the coordinate system  $(\xi_1, \xi_2, \xi_3)$ , we can

write  $v = v_1 e_1 + v_2 e_2 + v_3 e_3$ . After substituting  $h_3 = \epsilon$  one observes

$$\operatorname{div} v = \frac{1}{h_1 h_2} \left( \frac{\partial(h_2 v_1)}{\partial \xi_1} + \frac{\partial(h_1 v_2)}{\partial \xi_2} + \frac{1}{\epsilon} \frac{\partial(h_1 h_2 v_3)}{\partial \xi_3} \right). \quad (40)$$

Next, computing the components of the rate-of-strain tensor  $D[v] = \frac{1}{2}(\nabla v + \nabla v^T)$  we get

$$D[v]_{11} = \frac{1}{h_1} \frac{\partial v_1}{\partial \xi_1} + \frac{v_2}{h_1 h_2} \frac{\partial h_1}{\partial \xi_2} + \frac{v_3}{h_1 h_3} \frac{\partial h_1}{\partial \xi_3}, \quad D[v]_{23} = \frac{h_2}{2h_3} \frac{\partial}{\partial \xi_3} \left( \frac{v_2}{h_2} \right) + \frac{h_3}{2h_2} \frac{\partial}{\partial \xi_2} \left( \frac{v_3}{h_3} \right),$$

with the remaining components obtained by cyclic interchange of indices. Now, we take into account that the ratios  $\frac{v_\alpha}{v_3}$  scale like  $\epsilon$  due to the incompressibility constraint  $\operatorname{div} v = 0$  and (40), which reveals that

$$D[v]_{\alpha 3} = D[v]_{3\alpha} = \frac{\lambda_\alpha}{2\epsilon} \frac{\partial}{\partial \xi_3} \left( \frac{v_\alpha}{\lambda_\alpha} \right) + O(\epsilon)$$

with  $\alpha = 1, 2$  dominate the rest of the components. Thus, we finally obtain

$$\begin{aligned} \|D[v]\|_F^2 &= \sum_{ij} (D[v]_{ij})^2 = 2 \frac{1}{4\epsilon^2} \left| \Lambda \frac{\partial}{\partial \xi} (\Lambda^{-1} v_\Gamma) \right|_\Gamma^2 + O(1) \\ &= \frac{1}{2\epsilon^2} \left| (\operatorname{id} - \epsilon \xi S) \frac{\partial}{\partial \xi} ((\operatorname{id} + \epsilon \xi S + O(\epsilon^2)) v_\Gamma) \right|_\Gamma^2 + O(1) \\ &= \frac{1}{2\epsilon^2} \left| \frac{\partial v_\Gamma}{\partial \xi} + \epsilon S v_\Gamma \right|_\Gamma^2 + O(1), \end{aligned}$$

which leads to the expression in (4).

## B The 4th-order PDE Derived from the Gradient Flow.

Here, we verify the claim stated in Section 2.4 that the fourth order parabolic PDE (17) deduced from the gradient flow formulation coincides up to higher order terms in  $\epsilon$  with the PDE (18) derived by Roy, Roberts, and Simpson[39].

We recall that  $\hat{g} = -\nabla \mathbf{z}$ . Since  $\phi_0$  is an isometry, it is straightforward to show that  $\nabla \mathbf{z}(\mathbf{x}) = d\phi_0(\operatorname{grad}_\Gamma z(x)) + \langle \nabla \mathbf{z}(\mathbf{x}), n(x) \rangle n(x)$ , where  $\mathbf{x} = \phi_0(x)$  and  $z = \mathbf{z} \circ \phi$  is the pullback of  $\mathbf{z}$  onto  $\Gamma$ . Comparing with (2), we deduce that  $\hat{g}_\Gamma = -\operatorname{grad}_\Gamma z$  and  $\hat{g}_n(x) = -\langle \nabla \mathbf{z}(\mathbf{x}), n(x) \rangle$  and so  $\hat{g}_n = -\cos \theta$ . Furthermore, from  $u = h - \frac{\epsilon}{2} H h^2 + \frac{\epsilon^2}{3} K h^3$  we obtain, by inverting,  $h = u + \frac{\epsilon}{2} H u^2 + O(\epsilon^2)$ . This allows us to replace, as in Section 2, the height  $h$  with the mass concentration

$u$  in (18). For the first term on the right-hand side of (18), we get

$$\begin{aligned}
& -\frac{1}{3}h^2u \operatorname{grad}_\Gamma \tilde{H} + \frac{\epsilon}{6}h^4(H \operatorname{id} - S) \operatorname{grad}_\Gamma H \\
& = \left( \frac{1}{3}h^2u \operatorname{id} - \frac{\epsilon}{6}h^4(H \operatorname{id} - S) \right) \operatorname{grad}_\Gamma(-H) + \frac{1}{3}h^2u \operatorname{grad}_\Gamma(-\epsilon T u - \epsilon \Delta_\Gamma u) \\
& = (M(u) + \mathcal{O}(\epsilon^2)) \operatorname{grad}_\Gamma(-H) + (M(u) + \mathcal{O}(\epsilon)) \operatorname{grad}_\Gamma(-\epsilon T u - \epsilon \Delta_\Gamma u) \\
& = M(u) \operatorname{grad}_\Gamma(-H - \epsilon T u - \epsilon \Delta_\Gamma u) + \mathcal{O}(\epsilon^2),
\end{aligned}$$

and for the second term, we obtain

$$\begin{aligned}
& -\frac{\zeta}{3}h^3\hat{g}_\Gamma + \frac{\zeta\epsilon}{3}h^4(H \operatorname{id} + \frac{1}{2}S)\hat{g}_\Gamma - \frac{\zeta\epsilon}{3}\hat{g}_n h^3 \operatorname{grad}_\Gamma h \\
& = -\zeta \left( \frac{1}{3}h^3 \operatorname{id} - \frac{\epsilon}{3}h^4(H \operatorname{id} + \frac{1}{2}S) \right) \hat{g}_\Gamma - \zeta\epsilon\hat{g}_n \left( \frac{1}{3}h^3 \right) \operatorname{grad}_\Gamma h \\
& = -\zeta \left( \frac{1}{3}u^3 \operatorname{id} + \frac{\epsilon}{6}(H \operatorname{id} - S)u^4 + \mathcal{O}(\epsilon^2) \right) \hat{g}_\Gamma - \zeta\epsilon\hat{g}_n \left( \frac{1}{3}u^3 \operatorname{grad}_\Gamma u + \mathcal{O}(\epsilon) \right) \\
& = -\zeta \left( M(u) - \frac{\epsilon}{3}S u^4 \right) \hat{g}_\Gamma - \zeta\epsilon\hat{g}_n M(u) \operatorname{grad}_\Gamma u + \mathcal{O}(\epsilon^2) \\
& = -\zeta M(u)\hat{g}_\Gamma + \zeta\epsilon M(u)(uS\hat{g}_\Gamma) - \zeta\epsilon\hat{g}_n M(u) \operatorname{grad}_\Gamma u + \mathcal{O}(\epsilon^2) \\
& = \zeta M(u) (-\hat{g}_\Gamma + \epsilon u S \hat{g}_\Gamma - \epsilon \hat{g}_n \operatorname{grad}_\Gamma u) + \mathcal{O}(\epsilon^2) \\
& = \zeta M(u) (\operatorname{grad}_\Gamma z - \epsilon u \operatorname{grad}_\Gamma \hat{g}_n - \epsilon \hat{g}_n \operatorname{grad}_\Gamma u) + \mathcal{O}(\epsilon^2) \\
& = M(u) \operatorname{grad}_\Gamma (\zeta z + \zeta \epsilon \cos \theta u) + \mathcal{O}(\epsilon^2).
\end{aligned}$$

Here, we have used that  $\operatorname{grad}_\Gamma \hat{g}_n = -S\hat{g}_\Gamma$ . Indeed, consider a variation  $\delta x \in T_x\Gamma$  and take its product with the right-hand side. Using the definition of the (self-adjoint)  $S$ , as well as the fact that  $\hat{g}$  is constant and that  $d\phi_0(g_\Gamma) \perp n$ , we have

$$\langle -S\hat{g}_\Gamma, \delta x \rangle_\Gamma = \langle d\phi_0(\hat{g}_\Gamma), D_{\delta x} n \rangle = \langle \hat{g}, D_{\delta x} n \rangle = D_{\delta x} \langle \hat{g}, n \rangle = D_{\delta x} \hat{g}_n,$$

which is exactly the defining property of  $\operatorname{grad}_\Gamma \hat{g}_n$ , i.e.  $\langle \operatorname{grad}_\Gamma \hat{g}_n, \delta x \rangle_\Gamma = D_{\delta x} \hat{g}_n$  for any  $\delta x \in T_x\Gamma$ .

Now, summing the resulting two terms above we receive  $M(u) \operatorname{grad}_\Gamma \left( \frac{\delta E}{\delta u} \right) + \mathcal{O}(\epsilon^2)$  with  $M(u) = \frac{1}{3}u^3 \operatorname{id} + \frac{\epsilon}{6}u^4(H \operatorname{id} + S)$  and  $\frac{\delta E}{\delta u} = (\zeta z - H) + \epsilon(\zeta \cos \theta - T)u - \epsilon \Delta_\Gamma u$ . Hence, the model of Roy, Roberts and Simpson[39] (18) indeed agrees with the gradient flow PDE (17) up to  $\mathcal{O}(\epsilon^2)$ .

### Acknowledgements

Orestis Vantzos has been funded by the DFG via the Bonn International Graduate School in Mathematics and the Collaborative Research Center 611.

## References

- [1] J.W. Barrett, H. Garcke, and R. Nürnberg. Finite element approximation of surfactant spreading on a thin film. *SIAM Journal on Numerical Analysis*, 41(4):1472–1464, 2003.
- [2] G.K. Batchelor. *An introduction to fluid dynamics*. Cambridge mathematical library. Cambridge University Press, 2000.
- [3] E. Beretta, M. Bertsch, and R. Dal Passo. Nonnegative solutions of a fourth order nonlinear degenerate parabolic equation. *Arch. Rat. Mech. Anal.*, 129(2):175–200, 1995.
- [4] F. Bernis. Viscous flows, fourth order nonlinear degenerate parabolic equations and singular elliptic problems. In J.I. Diaz, M.A. Herrero, A. Linan, and J.L. Vazquez, editors, *Free boundary problems: theory and applications*, Pitman Research Notes in Mathematics 323, pages 40–56. Longman, Harlow, 1995.
- [5] F. Bernis and A. Friedman. Higher order nonlinear degenerate parabolic equations. *J. Diff. Equ.*, 83:179–206, 1990.
- [6] A.L. Bertozzi and M. Pugh. The lubrication approximation for thin viscous films: regularity and long time behaviour of weak solutions. *Communications on pure and applied mathematics*, 49(2):85–123, 1996.
- [7] M. Boutounet, L. Chupin, P. Noble, and J. P. Vila. Shallow water viscous flows for arbitrary topography. *Commun. Math. Sci.*, 6(1):29–55, 2008.
- [8] S.P. Boyd and L. Vandenberghe. *Convex optimization*. Cambridge University Press, 2004.
- [9] R. Braun, R. Usha, G. McFadden, T. Driscoll, L. Cook, and P. King-Smith. Thin film dynamics on a prolate spheroid with application to the cornea. *Journal of Engineering Mathematics*, pages 1–18. 10.1007/s10665-011-9482-4.
- [10] R. V. Craster and O. K. Matar. Dynamics and stability of thin liquid films. *Reviews of Modern Physics*, 81, 2009.
- [11] M. Desbrun, E. Kanso, and Y. Tong. Discrete differential forms for computational modeling. In G. M. Ziegler P. Schröder, J. M. Sullivan, editor, *Discrete Differential Geometry*, Oberwolfach Seminars, pages 287–324. Birkhäuser Basel, 2004.
- [12] Julia Dohmen, Natalie Grunewald, Felix Otto, and Martin Rumpf. *Mathematics - Key Technology for the Future*, chapter Micro Structures in Thin Coating Layers: Micro Structure Evolution and Macroscopic Contact Angle. Springer, 2007.

- [13] Bertram Düring, Daniel Matthes, and Josipa Pina Milišić. A gradient flow scheme for nonlinear fourth order equations. *Discrete Contin. Dyn. Syst. Ser. B*, 14(3):935–959, 2010.
- [14] Sharif Elcott, Yiyong Tong, Eva Kanso, Peter Schröder, and Mathieu Desbrun. Stable, circulation-preserving, simplicial fluids. In *SIGGRAPH '06: ACM SIGGRAPH 2006 Courses*, pages 60–68. ACM, 2006.
- [15] Sharif Elcott, Yiyong Tong, Eva Kanso, Peter Schröder, and Mathieu Desbrun. Stable, circulation-preserving, simplicial fluids. In *ACM SIGGRAPH ASIA 2008 courses*, SIGGRAPH Asia '08, pages 17:1–17:11, New York, NY, USA, 2008. ACM.
- [16] Th. Frankel. *The Geometry of Physics: An Introduction*. Cambridge University Press, 2nd edition, 2004.
- [17] L. Giacomelli and F. Otto. Rigorous lubrication approximation. *Interfaces and Free boundaries*, 5(4):481–529, 2003.
- [18] Lorenzo Giacomelli and Felix Otto. Droplet spreading: intermediate scaling law by PDE methods. *Comm. Pure Appl. Math.*, 55(2):217–254, 2002.
- [19] K. B. Glasner. Variational models for moving contact lines and the quasi-static approximation. *European Journal of Applied Mathematics*, 16(06):713–740, 2005.
- [20] J. B. Greer, A. L. Bertozzi, and G. Sapiro. Fourth order partial differential equations on general geometries. *Journal of Computational Physics*, 216(1):216–246, 2006.
- [21] G. Grün and M. Rumpf. Nonnegativity preserving convergent schemes for the thin film equation. *Numerische Mathematik*, 87:113–152, 2000.
- [22] Günther Grün, Martin Lenz, and Martin Rumpf. A finite volume scheme for surfactant driven thin film flow. In R. Herbin and D. Kröner, editors, *Finite Volumes for Complex Applications III*, pages 567–574. Hermes Penton Sciences, 2002.
- [23] Anil N. Hirani. *Discrete Exterior Calculus*. PhD thesis, California Institute of Technology, May 2003.
- [24] Anil N. Hirani, Kalyana B. Nakshatrala, and Jehanzeb H. Chaudhry. Numerical method for Darcy flow derived using Discrete Exterior Calculus. Technical Report UIUCDCS-R-2008-2937, Department of Computer Science, University of Illinois at Urbana-Champaign, October 2008. Also available as a preprint at arXiv as arXiv:0810.3434v3 [math.NA].
- [25] P.D. Howell. Surface-tension-driven flow on a moving curved surface. *Journal of Engineering Mathematics*, 45:283–308, 2003. 10.1023/A:1022685018867.

- [26] O. E. Jensen, G. P. Chini, and J. R. King. Thin-film flows near isolated humps and interior corners. *Journal of Engineering Mathematics*, 50:289–309, 2004.
- [27] S. Kalliadasis and C. Bielarz. Steady free-surface thin film flows over topography. *Physics of Fluids*, 12(8), 2000.
- [28] Martin Lenz, Simplice Firmin Nmadjieu, and Martin Rumpf. A convergent finite volume scheme for diffusion on evolving surfaces. *SIAM Journal on Numerical Analysis*, 49(1):15–37, 2011.
- [29] J. R. Lister, J. M. Rallison, and S. J. Rees. The nonlinear dynamics of pendent drops on a thin film coating the underside of a ceiling. *Journal of Fluid Mechanics*, 647:239–264, 2010.
- [30] Daniel Matthes, Robert J. McCann, and Giuseppe Savaré. A family of nonlinear fourth order equations of gradient flow type. *Comm. Partial Differential Equations*, 34(10-12):1352–1397, 2009.
- [31] T. G. Myers. Thin films with high surface tension. *SIAM Rev.*, 40(3):441–462, 1998.
- [32] T. G. Myers, J. P. F. Charpin, and S. J. Chapman. The flow and solidification of a thin fluid film on an arbitrary three-dimensional surface. *Phys. Fluids*, 14(8):2788–2803, 2002.
- [33] Johannes C. C. Nitsche. *Lectures on Minimal Surfaces: Volume 1, Introduction, Fundamentals, Geometry and Basic Boundary Value Problems*. Cambridge University Press, 1989.
- [34] A. Oron, S.H. Davis, and S.G. Bankoff. Long-scale evolution of thin liquid films. *Rev. of Mod. Phys.*, 69:931–980, 1997.
- [35] Felix Otto. The geometry of dissipative evolution equations: the porous medium equation. *Comm. Partial Differential Equations*, 26(1-2):101–174, 2001.
- [36] C. Pozrikidis. *Introduction to theoretical and computational fluid dynamics*. Topics in Chemical Engineering Series. Oxford University Press, 1997.
- [37] O. Reynolds. On the theory of lubrication and its application to Mr. Beauchamp Tower’s experiments, including an experimental determination of the viscosity of olive oil. *Philos. Trans. R. Soc. London*, 177:157–234, 1886.
- [38] A. J. Roberts and Z. Li. An accurate and comprehensive model of thin fluid flows with inertia on curved substrates. *Journal of Fluid Mechanics*, 553(1):33–73, 2006.

- [39] R. Valéry Roy, A. J. Roberts, and M. E. Simpson. A lubrication model of coating flows over a curved substrate in space. *J. Fluid Mech.*, 454:235–261, 2002.
- [40] Bidyut Santra and Bhabani Dandapat. Thin-film flow over a nonlinear stretching sheet. *Zeitschrift für Angewandte Mathematik und Physik (ZAMP)*, 60:688–700, 2009. 10.1007/s00033-008-8015-0.
- [41] L. W. Schwartz and D. E. Weidner. Modeling of coating flows on curved surfaces. *Journal of Engineering Mechanics*, 29:91–103, 1995.
- [42] Dejan Slepčev. Linear stability of selfsimilar solutions of unstable thin-film equations. *Interfaces Free Bound.*, 11(3):375–398, 2009.
- [43] D. Takagi and H. E. Huppert. Flow and instability of thin films on a cylinder and sphere. *J. Fluid Mech.*, 647:221–238, 2010.
- [44] J. Thiffeault and K. Kamhawi. Transport in thin gravity-driven flow over a curved substrate. arXiv:nlin/0607075v1 [nlin.CD], 2006.
- [45] Cédric Villani. *Topics in Optimal Transportation*. Mathematical Surveys and Monographs. American Mathematical Society, Providence, RI, 2003.
- [46] C. Y. Wang. Thin film flowing down a curved surface. *Zeitschrift für Angewandte Mathematik und Physik (ZAMP)*, 35:532–544, 1984. 10.1007/BF00945073.
- [47] Jian-Jun Xu, Zhilin Li, John Lowengrub, and Hongkai Zhao. A level-set method for interfacial flows with surfactant. *J. Comp. Phys.*, 212:590–616, 2006.
- [48] Hiroaki Yoshimura and Jerrold E. Marsden. Dirac structures in Lagrangian mechanics part ii: Variational structures. *Journal of Geometry and Physics*, 57(1):209–250, 2006.
- [49] L. Zhornitskaya and A.L. Bertozzi. Positivity preserving numerical schemes for lubrication-type equations. *SIAM Journal on Numerical Analysis*, 37(2):523–555, 2000.